

# Sampling and Super-resolution of Sparse Signals Beyond the Fourier Domain

Ayush Bhandari and Yonina C. Eldar

## Abstract

Recovering a sparse signal from its low-pass projections in the Fourier domain is a problem of broad interest in science and engineering and is commonly referred to as super-resolution. In many cases, however, Fourier domain may not be the natural choice. For example, in holography, low-pass projections of sparse signals are obtained in the Fresnel domain. Similarly, time-varying system identification relies on low-pass projections on the space of linear frequency modulated signals. In this paper, we study the recovery of sparse signals from low-pass projections in the Special Affine Fourier Transform domain (SAFT). The SAFT parametrically generalizes a number of well known unitary transformations that are used in signal processing and optics. In analogy to the Shannon's sampling framework, we specify sampling theorems for recovery of sparse signals considering three specific cases: (1) sampling with arbitrary, bandlimited kernels, (2) sampling with smooth, time-limited kernels and, (3) recovery from Gabor transform measurements linked with the SAFT domain. Our work offers a unifying perspective on the sparse sampling problem which is compatible with the Fourier, Fresnel and Fractional Fourier domain based results. In deriving our results, we introduce the SAFT series (analogous to the Fourier series) and the short time SAFT, and study convolution theorems that establish a convolution–multiplication property in the SAFT domain.

Preliminary ideas leading to this manuscript were presented in parts at ICASSP 2015 [1] and 2016 [2].

A. Bhandari is with the Massachusetts Institute of Technology, Cambridge, MA 02139-4307 USA. e-mail: ayush@MIT.edu.

Y. Eldar is with the Technion–Israel Institute of Technology, Haifa 32000, Israel. e-mail: yonina@ee.technion.ac.il.

The work of Y. Eldar was funded by the European Union's Horizon 2020 research and innovation program under grant agreement ERC-BNYQ, by the Israel Science Foundation under Grant no. 335/14, and by ICore: the Israeli Excellence Center 'Circle of Light'.

Manuscript received Month XX, 20XX; revised Month XX, 20XX.

## CONTENTS

<b>I</b>	<b>Introduction</b>	3
<b>II</b>	<b>The Special Affine Fourier Transform</b>	6
II-A	Forward Transform . . . . .	7
II-B	Inverse Transform . . . . .	9
II-C	Geometry of the Special Affine Fourier Transform . . . . .	10
II-D	Convolution Structures in the SAFT Domain . . . . .	14
<b>III</b>	<b>SAFT Domain and Bandlimited Subspaces</b>	16
<b>IV</b>	<b>Sparse Sampling and Super-resolution</b>	18
IV-A	Special Affine Fourier Series (SAFS) . . . . .	19
IV-B	Sparse Signals and Arbitrary Bandlimited Kernels . . . . .	23
IV-C	Generalization to Arbitrary Bandlimited Sampling Kernels . . . . .	25
IV-D	Special cases of the SAFT domain result . . . . .	26
IV-E	Sparse Signals and Smooth Time-limited Kernels . . . . .	28
IV-F	Sparse Signals and the Gabor Transform Kernel . . . . .	30
<b>V</b>	<b>Conclusion</b>	32
<b>VI</b>	<b>Appendix: Auxiliary Proofs and Computations</b>	33
VI-A	Proof of Proposition 1 . . . . .	33
VI-B	Proof of Proposition 2 . . . . .	34
VI-C	Proof of Proposition 3 . . . . .	35
VI-D	Proof of Proposition 4 . . . . .	36
	<b>References</b>	37

## I. INTRODUCTION

**T**HE problem of super-resolution deals with recovery of spikes or Dirac masses from low-pass projections in the Fourier domain. This is a standard problem with numerous applications in science and engineering. In this setting, the measurements amount to a stream of smooth pulses where the low-pass nature is due to the pulse shape. This may be an excitation pulse used in time-of-flight imaging such as radar, sonar, lidar and ultrasound. The pulse shape may also be represented as a low-pass filter that is an approximation of,

- point spread function of an optical instrument such as a lens, microscope or a telescope.
- transfer function of an electronic sensor such as an antenna or a microphone.
- Green's function of some partial differential equation that represents a physical process (for example, diffusion or fluorescence lifetime imaging).
- beampattern of a sensor array.
- spectral line shape in spectroscopy (often assumed to be a Cauchy, Gaussian or a Voigt distribution).

Several well known signal processing applications involve super-resolution [3]–[5] including source localization [6], time-delay estimation [7]–[10], sparse deconvolution [11] and, time-of-flight imaging (e.g. optical [12]–[14], radar [15]–[17] and ultrasound [18], [19]). These applications all address the same challenge: “*How can one recover a signal with broadband features (spikes) from a given set of narrowband measurements?*”

Our problem can be restated as that of uniform sampling and recovery of spikes with a given bandlimited kernel. Unlike bandlimited or smooth signals which follow a linear recovery principle [20], [21], sparse signals rely on non-linear recovery method. Despite the prevalence of the spike recovery problem across several fields (cf. Table I and Table II in [8], [9] as well as [11]), the link to sampling theory was established only recently by Vetterli [22], Blu [23] and co-workers in their study of *finite rate of innovation* or FRI signals. These are signals which are described by countable degrees of freedom, per unit time and model a broad class of signals. The FRI sampling has been

applied to a number of interesting applications such as channel estimation [24], radar [15]–[17], time-resolved imaging [14], [17], [25], sparse recovery on a sphere [26], image feature detection [27]–[29], medical imaging [18], [19], [30], [31], tomography [32], astronomy [33], spectroscopy [34], unlimited sampling architecture [35], [36] and inverse source problems [37], [38].

In either case, super-resolution or sampling of sparse signals, a common feature is that both problems assume a bandlimited kernel. The choice of Fourier domain for defining bandlimitedness may be restrictive. In practice, many systems and physical phenomena are modeled as linear and time-varying/non-stationary. On the other hand, complex exponentials—that are constituent components of the Fourier transform—are the eigenfunctions of linear time-invariant systems. Polynomial phase models [39]–[41] that generalize complex exponentials are often used as an alternative basis for modeling time-varying systems. Such models are specified by basis functions of the form  $e^{j\varphi(t)}$ . One notable example is that of quadratic chirps which are specified by  $\varphi(t) = a_2t^2 + a_1t + a_0$ . Due to their wide applicability, chirp based transformations [42], multi-scale orthonormal bases and frames [43] as well as dictionary based pursuit algorithms [44] have been derived in the literature. Active imaging systems such as radar [45] and sonar [46] use chirps for probing the environment. In [47], Martone demonstrates the use of polynomial phase basis functions of the fractional Fourier transform for multicarrier communication with time-frequency selective channels. Harms *et al.* [48] use chirps for identification of linear time-varying systems. Besides chirps, Fresnel transforms [49] use polynomial phase representation for digital holography [50] and diffraction. Other applications of polynomial phase functions include time-frequency representations [51], DOA estimation [40], sensor array processing [41], [52], ghost imaging [53], image encryption [54] and quantum physics [55].

Polynomial phase representations were also studied in the context of phase space and mathematical physics. This led to the development of unitary transformations such as the fractional Fourier transform (FrFT) [56] and the Linear Canonical Transform (LCT) [57], [58]. These transformations generalize the Fourier transform in the same way that polynomial phase functions  $e^{j\varphi(t)}$  generalizes the complex exponentials, or  $e^{j\omega t}$ .

In the area of signal processing, Almeida first introduced the fractional Fourier transform (FrFT) as a tool for time-frequency representations [59]. Following [59], a number of papers have extended the Shannon's sampling theorem to the FrFT domain (cf. [60] and [61] and references there in). In [61], Bhandari and Zayed developed the shift-invariant model for the FrFT domain which was later extended in [62], [63]. Sampling of sparse signals in the FrFT domain was studied in [64]. Interestingly, all of the aforementioned transformations and corresponding basis functions are specific cases of the Special Affine Fourier Transform (SAFT).

In this paper, our goal is to extend sampling theory of sparse signals beyond the Fourier domain. We do so by considering the SAFT which is a parametric transformation that subsumes a number of well known unitary transformations used in signal processing and optics. We recently studied sampling theory of bandlimited and smooth signals in the SAFT domain in [63]. By using results developed in [63], here we derive sampling theorems for sparse signals with three distinct flavors:

- 1) Sampling with arbitrary, bandlimited kernels.
- 2) Sampling with smooth, time-limited kernels.
- 3) Sparse signal recovery from Gabor transform measurements linked with the SAFT domain.

For this purpose, we introduce two mathematical tools:

- the Special Affine Fourier Series (a generalization of the Fourier Series) for representing time-limited functions.
- the Gabor transform associated with the SAFT (a generalization of the usual Gabor transform).

We begin with the definition of the SAFT in Section II. The forward transform, its inverse as well as geometric properties are discussed in the subsections that follow. In order to develop sparse sampling theory for the SAFT, in Section II-D we recall convolution operators for the SAFT domain [65]. This allows us to establish the link between convolution and low-pass orthogonal projection operators. We then recall Shannon's sampling theorem for SAFT bandlimited functions [65] in Section III. Our main results on sparse sampling theory are presented in Section IV where we discuss three cases. Unlike the Fourier basis functions, the SAFT counterparts are aperiodic. As a workaround, in Section IV-A,

we develop the Special Affine Fourier Series (SAFS) for time-limited signals. The SAFS is then used to represent sparse signals and we conclude this work with several future directions in Section V.

Throughout the paper, set of integers, reals and complex numbers is denoted by  $\mathbb{Z}, \mathbb{R}$ , and  $\mathbb{C}$ , respectively and  $\mathbb{Z}^+$  denotes a set of positive integers. Continuous-time functions are denoted by  $f(t), t \in \mathbb{R}$  while  $f[m], m \in \mathbb{Z}$  are used for their discrete counterparts. We use script fonts for operators, that is,  $\mathcal{O}f$ . For instance,  $\mathcal{P}$  denotes the projection operator and the derivative operator of order  $k$  is written as  $\mathcal{D}^k f = f^{(k)}$ . Function/operator composition is denoted by  $\circ$ . We use boldface font for representing vectors and matrices, for example  $\mathbf{x}$  and  $\mathbf{X}$ , respectively, and  $\mathbf{X}^\top$  is the matrix transpose. We use  $\mathbf{I}$  to denote an identity matrix. A characteristic function on domain  $\mathcal{D}$  is denoted by  $\mathbb{1}_{\mathcal{D}}$ . Dirac distribution is represented by  $\delta(t), t \in \mathbb{R}$ . All operations linked with  $\delta$  are treated in terms of distributions. The Kronecker delta is represented by  $\delta[m], m \in \mathbb{Z}$ . The space of square-integrable and absolutely integrable functions is denoted by  $L_2$  and  $L_1$ , respectively and  $\langle f, g \rangle = \int fg^*$  is the  $L_2$  inner-product. We use  $\overline{(\cdot)}$  to denote time-reversal.

## II. THE SPECIAL AFFINE FOURIER TRANSFORM

The Special Affine Fourier Transform or the SAFT was introduced by Abe and Sheridan [66] as a generalization of the FrFT. The SAFT can be thought of as a versatile transformation which parametrically generalizes a number of well known unitary and non-unitary transformations as well as mathematical and optical operations. In Table I we list its parameters together with the associated mappings.

TABLE I  
SAFT, TRANSFORMATIONS AND OPERATIONS

SAFT Parameters ( $\Lambda_S$ )	Corresponding Transform
$\begin{bmatrix} 0 & 1 & 0 \\ -1 & 0 & 0 \end{bmatrix} = \Lambda_{\text{FT}}$	<b>Fourier Transform (FT)</b>
$\begin{bmatrix} 0 & 1 & p \\ -1 & 0 & q \end{bmatrix} = \Lambda_{\text{FT}}^{\circ}$	<b>Offset Fourier Transform</b>
$\begin{bmatrix} \cos \theta & \sin \theta & 0 \\ -\sin \theta & \cos \theta & 0 \end{bmatrix} = \Lambda_{\theta}$	<b>Fractional Fourier Transform (FrFT)</b>
$\begin{bmatrix} \cos \theta & \sin \theta & p \\ -\sin \theta & \cos \theta & q \end{bmatrix} = \Lambda_{\theta}^{\circ}$	<b>Offset Fractional Fourier Transform</b>
$\begin{bmatrix} a & b & 0 \\ c & d & 0 \end{bmatrix} = \Lambda_L$	<b>Linear Canonical Transform (LCT)</b>
$\begin{bmatrix} 1 & b & 0 \\ 0 & 1 & 0 \end{bmatrix} = \Lambda_{\text{Fr}}$	<b>Fresnel Transform</b>
$\begin{bmatrix} 0 & j & 0 \\ j & 0 & 0 \end{bmatrix} = \Lambda_{\text{LT}}$	<b>Laplace Transform (LT)</b>
$\begin{bmatrix} j \cos \theta & j \sin \theta & 0 \\ j \sin \theta & -j \cos \theta & 0 \end{bmatrix}$	<b>Fractional Laplace Transform</b>
$\begin{bmatrix} 1 & jb & 0 \\ j & 1 & 0 \end{bmatrix}$	<b>Bilateral Laplace Transform</b>
$\begin{bmatrix} 1 & -jb & 0 \\ 0 & 1 & 0 \end{bmatrix}, b \geq 0$	<b>Gauss-Weierstrass Transform</b>
$\frac{1}{\sqrt{2}} \begin{bmatrix} 0 & e^{-j\pi/2} \\ -e^{-j\pi/2} & 1 \end{bmatrix}$	<b>Bargmann Transform</b>
SAFT Parameters ( $\Lambda_S$ )	Corresponding Signal Operation
$\begin{bmatrix} 1/\alpha & 0 & 0 \\ 0 & \alpha & 0 \end{bmatrix} = \Lambda_{\alpha}$	<b>Time Scaling</b>
$\begin{bmatrix} 1 & 0 & \tau \\ 0 & 1 & 0 \end{bmatrix} = \Lambda_{\tau}$	<b>Time Shift</b>
$\begin{bmatrix} 1 & 0 & 0 \\ 0 & 1 & \xi \end{bmatrix} = \Lambda_{\xi}$	<b>Frequency Shift/Modulation</b>
SAFT Parameters ( $\Lambda_S$ )	Corresponding Optical Operation
$\begin{bmatrix} \cos \theta & \sin \theta & 0 \\ -\sin \theta & \cos \theta & 0 \end{bmatrix} = \Lambda_{\theta}$	<b>Rotation</b>
$\begin{bmatrix} 1 & 0 & 0 \\ \tau & 1 & 0 \end{bmatrix} = \Lambda_{\tau}$	<b>Lens Transformation</b>
$\begin{bmatrix} 1 & \eta & 0 \\ 0 & 1 & 0 \end{bmatrix} = \Lambda_{\eta}$	<b>Free Space Propagation</b>
$\begin{bmatrix} e^{\beta} & 0 & 0 \\ 0 & e^{-\beta} & 0 \end{bmatrix} = \Lambda_{\beta}$	<b>Magnification</b>
$\begin{bmatrix} \cosh \alpha & \sinh \alpha & 0 \\ \sinh \alpha & \cosh \alpha & 0 \end{bmatrix} = \Lambda_{\eta}$	<b>Hyperbolic Transformation</b>

### A. Forward Transform

Mathematically, the SAFT of a signal  $f(t)$  is a mapping,  $\mathcal{T}_{\text{SAFT}} : f \rightarrow \hat{f}_{\Lambda_S}$  which is defined by an integral transformation parameterized by a matrix  $\Lambda_S$

$$\mathcal{T}_{\Lambda_S} [f] = \hat{f}_{\Lambda_S}(\omega) = \begin{cases} \langle f, \kappa_{\Lambda_S}(\cdot, \omega) \rangle & b \neq 0 \\ \sqrt{d} e^{j\frac{cd}{2}(\omega-p)^2 + j\omega q} f(d(\omega-p)) & b = 0. \end{cases} \quad (1)$$

When  $b \neq 0$ , the matrix  $\Lambda_S^{(2 \times 3)}$  is the SAFT parameter matrix,

$$\Lambda_S = \left[ \begin{array}{cc|c} a & b & p \\ c & d & q \end{array} \right] \equiv \left[ \Lambda_L \mid \boldsymbol{\lambda} \right], \quad (2)$$

which is obtained by concatenating the Linear Canonical Transform or the LCT matrix,

$$\Lambda_L = \begin{bmatrix} a & b \\ c & d \end{bmatrix}, \quad |\Lambda_L| = 1 \text{ or } ad - bc = 1$$

(see Table I and [57]), and, an offset vector,  $\boldsymbol{\lambda} = [p \ q]^\top$  with elements  $p$  and  $q$  that represent displacement and modulation, respectively. Let  $\mathbf{r} = [t \ \omega]^\top$  denote the time-frequency co-ordinates. The function  $\kappa_{\Lambda_S}(\mathbf{r})$  in (1) is the parametric SAFT kernel based on a complex exponential of quadratic form,

$$\kappa_{\Lambda_S}(\mathbf{r}) = K_{\Lambda_S}^* \exp\left(-j\left(\mathbf{r}^\top \mathbf{U} \mathbf{r} + \mathbf{v}^\top \mathbf{r}\right)\right) \quad (3)$$

where,

$$\mathbf{U} = \frac{1}{2b} \begin{bmatrix} a & -1 \\ -1 & d \end{bmatrix}, \quad \mathbf{v} = \frac{1}{b} \begin{bmatrix} p \\ bq - dp \end{bmatrix} \quad \text{and} \quad K_{\Lambda_S} = \frac{1}{\sqrt{j2\pi b}} \exp\left(j\frac{dp^2}{2b}\right).$$

Both  $\mathbf{U}$  and  $\mathbf{v}$  are parameterized by  $\Lambda_S$  and hence the SAFT kernel is also parameterized by  $\Lambda_S$ .

The exponential part of the kernel is explicitly written as,

$$\exp\left(-j\left(\mathbf{r}^\top \mathbf{U} \mathbf{r} + \mathbf{v}^\top \mathbf{r}\right)\right) = \exp\left(-\frac{j}{2b}\left(at^2 + d\omega^2 + 2t(p - \omega) - 2\omega(dp - bq)\right)\right).$$

Note that  $\Lambda_L$  has 3 free parameters  $\{a, b, d\}$  and  $c$  is constrained by  $|\Lambda_L| = 1$ . Due to this concatenation of the LCT matrix with a vector, the SAFT is also referred to as the *Offset Linear Canonical Transform* or the OLCT [67]. The matrix  $\Lambda_S$  arises naturally in applications involving optics and imaging. We refer the reader to the books [58], [68] for further details on the intuitive



meaning of such a matrix representation.

The SAFT of the Dirac distribution is calculated by,

$$\begin{aligned}\widehat{\delta}_{\Lambda_S}(\omega) &\stackrel{(1)}{=} \langle \delta, \kappa_{\Lambda_S}(\cdot, \omega) \rangle \\ &= \kappa_{\Lambda_S}^*(t, \omega)|_{t=0} \\ &= K_b \exp\left(\frac{j}{2b}(d\omega^2 - 2\omega(dp - bq))\right),\end{aligned}\tag{4}$$

and is non-bandlimited.

### B. Inverse Transform

In order to define the inverse-SAFT, we first note that the SAFT satisfies the following composition property,

$$(\mathcal{T}_{\Lambda_{S_2}} \circ \mathcal{T}_{\Lambda_{S_1}})[f] = z_0 \mathcal{T}_{\Lambda_{S_3}}[f]\tag{5}$$

where  $z_0$  is a complex number (phase offset). The elements of the resultant SAFT parameter matrix are specified by,

$$\Lambda_{S_3} = \left[ \Lambda_{L_3} \mid \lambda_3 \right] = \left[ \Lambda_{L_2} \Lambda_{L_1} \mid \Lambda_{L_2} \lambda_2 + \lambda_1 \right].$$

In the context of phase space, the physical significance of the SAFT parameter matrix is that it maps time-frequency co-ordinates  $\mathbf{r} = [t \ \omega]^\top$  into its affine transformed version,

$$\begin{bmatrix} t \\ \omega \end{bmatrix} \xrightarrow{\text{SAFT}} \begin{bmatrix} a & b \\ c & d \end{bmatrix} \begin{bmatrix} t \\ \omega \end{bmatrix} + \begin{bmatrix} p \\ q \end{bmatrix} \equiv \mathbf{r} \xrightarrow{\text{SAFT}} \Lambda_L \mathbf{r} + \boldsymbol{\lambda}.$$

Hence, the inverse-SAFT is defined by some affine transform that allows for the mapping,

$$\begin{bmatrix} at + bp + p \\ ct + d\omega + q \end{bmatrix} \xrightarrow{\text{Inverse SAFT}} \begin{bmatrix} t \\ \omega \end{bmatrix}.$$

Thanks to the composition property (5), setting,

$$\begin{aligned}\Lambda_{S_3} &= \begin{bmatrix} \Lambda_{L_3} & \lambda_3 \end{bmatrix} = \begin{bmatrix} \mathbf{I} & \mathbf{0} \end{bmatrix} \quad (\text{Identity Operation}) \\ \Rightarrow \Lambda_{L_2} &= \Lambda_{L_1}^{-1} \quad \text{and} \quad \lambda_2 = -\Lambda_{L_2} \lambda_1,\end{aligned}$$

results in the inverse parameter matrix defining inverse-SAFT which is equivalent to an SAFT with matrix  $\Lambda_S^{\text{inv}}$ ,

$$\Lambda_S^{\text{inv}} = \left[ \begin{array}{cc|cc} +d & -b & bq - dp & \\ -c & +a & cp - aq & \end{array} \right] = \begin{bmatrix} \Lambda_L^{-1} & -\Lambda_L^{-1} \lambda \end{bmatrix} \quad (6)$$

where  $c = \frac{ad-1}{b}$ . Thus, the inverse transform (iSAFT) is defined as an SAFT with matrix  $\Lambda_S^{\text{inv}}$  in (6),

$$\mathcal{T}_{\Lambda_S^{\text{inv}}}[f] = f(t) = K_{\Lambda_S^{\text{inv}}} \left\langle \widehat{f}_{\Lambda_S}, \kappa_{\Lambda_S^{\text{inv}}}(\cdot, t) \right\rangle \quad (7)$$

where  $\kappa_{\Lambda_S^{\text{inv}}}(\omega, t) = \kappa_{\Lambda_S}^*(t, \omega)$  and,

$$K_{\Lambda_S^{\text{inv}}} = \exp\left(\frac{j}{2}(cdp^2 + abq^2 - 2adpq)\right).$$

### C. Geometry of the Special Affine Fourier Transform

An intriguing property of the SAFT is its geometrical interpretation in the context of time-frequency representations and the fact that the parameter matrix belongs to a class of area preserving matrices—the ones whose determinant is unity. We elaborate on these aspects starting with the cyclic property of the Fourier transform [56].

Let  $\mathcal{T}_{\Lambda_{\text{FT}}}^{(0)} = \mathbf{I}$  be the identity operation that is,  $\mathcal{T}_{\Lambda_{\text{FT}}}^{(0)}[f] = f$  which we use to define the Fourier operator composition:

$$\mathcal{T}_{\Lambda_{\text{FT}}}^{(k)} = \mathcal{T}_{\Lambda_{\text{FT}}}^{(k-1)} \circ \mathcal{T}_{\Lambda_{\text{FT}}} = \underbrace{\mathcal{T}_{\Lambda_{\text{FT}}} \circ \dots \circ \mathcal{T}_{\Lambda_{\text{FT}}}}_{k\text{-times}}, \quad k \in \mathbb{Z}^+. \quad (8)$$

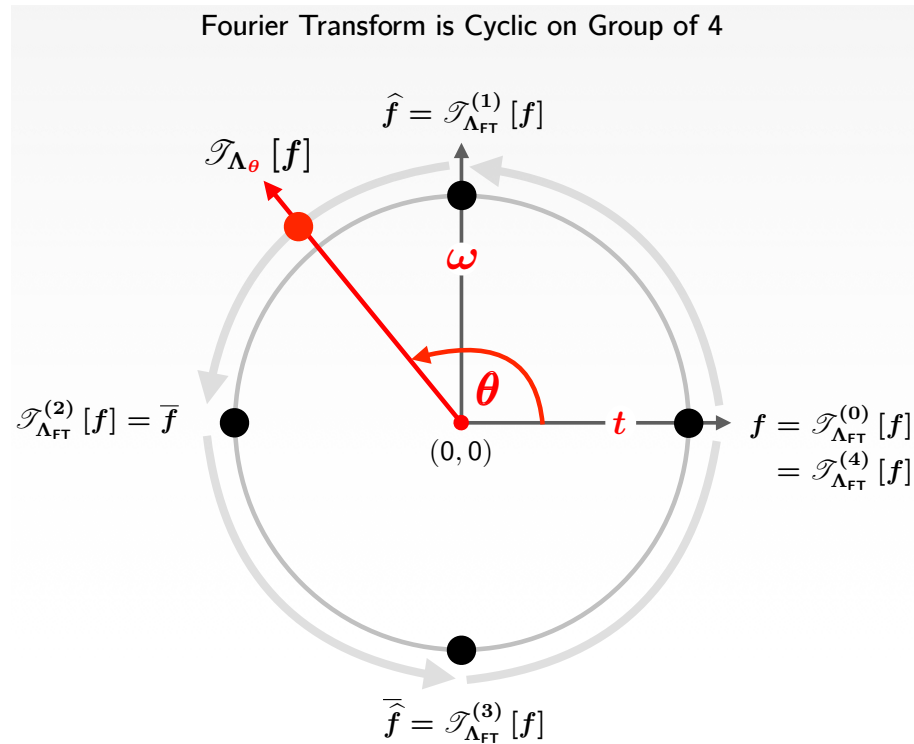


Fig. 1. Fourier transform is cyclic on a group of 4, that is,  $\mathcal{T}_{\Lambda_{\text{FT}}}^{(k+4)} = \mathcal{T}_{\Lambda_{\text{FT}}}^{(k)}, k \in \mathbb{Z}^+$  as described in (8). The Fractional Fourier transform allows for “fractionalization” of  $k$  so that a version of the Fourier transform may be defined on an arbitrary point on the circle. We denote such as transform by  $\mathcal{T}_{\Lambda_\theta}[f], \theta \in \mathbb{R}$ .

Note that:

$$\begin{aligned}
 \hat{f} &= \mathcal{T}_{\Lambda_{\text{FT}}}^{(1)}[f] & \bar{f} &= \mathcal{T}_{\Lambda_{\text{FT}}}^{(2)}[f] \\
 \bar{\bar{f}} &= \mathcal{T}_{\Lambda_{\text{FT}}}^{(3)}[f] & f &= \underbrace{\mathcal{T}_{\Lambda_{\text{FT}}}^{(4)}[f]}_{\text{Identity Operation}} \equiv \mathcal{T}_{\Lambda_{\text{FT}}}^{(0)}[f].
 \end{aligned}$$

From the last equality,  $\mathcal{T}_{\Lambda_{\text{FT}}}^{(4)}[f] = \mathcal{T}_{\Lambda_{\text{FT}}}^{(0)}[f]$ , we conclude that the Fourier operator is periodic with  $N = 4$ . Due to this periodic structure, the Fourier operator can be represented on a circle as shown in Fig. 1.

Unitary mappings that can be continuously defined on the circle (as opposed to  $k \in \mathbb{Z}^+$ ) were first identified by Condon [56]. This is known as the fractional Fourier transform (FrFT). Qualitatively, the FrFT “fractionalizes” the Fourier transform in the sense that  $\mathcal{T}_{\Lambda_{\text{FT}}}^{(k)}[f], k \in \mathbb{Z}^+$  can be defined

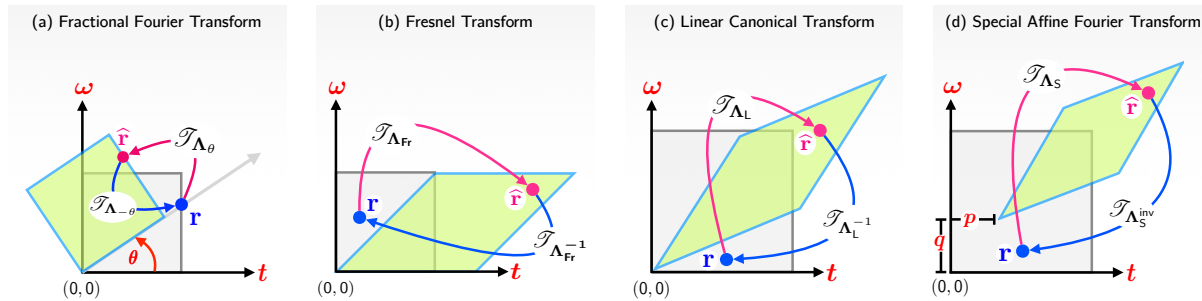


Fig. 2. The SAFT maps one convex enclosure into another while preserving area since the transformation matrix  $\Lambda_L \in \text{SL}_2(\mathbb{R})$ . The action of  $\Lambda_L$  on a time-frequency co-ordinate  $\mathbf{r} \in \mathbb{R}^2$  ( $[0, 1]$ ) results in  $\hat{\mathbf{r}} = \Lambda_L \mathbf{r}$ . (a) For the FrFT,  $\Lambda_L = \Lambda_\theta$  implements rotation. The inverse transform corresponds to  $\Lambda_\theta^{-1} = \Lambda_\theta^\top$ . (b) For the Fresnel transform,  $\Lambda_L = \Lambda_{\text{Fr}}$  implements shear. The inverse transform corresponds to  $\Lambda_{\text{Fr}}^{-1}$ . (c) For the Linear Canonical Transform (LCT),  $\Lambda_L$  deforms a unit square into an arbitrary parallelogram. The inverse transform corresponds to  $\Lambda_L^{-1}$ . (d) For the SAFT, presence of an offset  $\lambda = [p \ q]^\top$  results in an affine transform. Consequently, the inverse transform is  $\mathbf{r} = \Lambda_L^{-1} \hat{\mathbf{r}} - \Lambda_L^{-1} \lambda$ .

for an arbitrary point on the circle through  $\theta = k\pi/2, k \in \mathbb{Z}$  by the transformation  $\mathcal{T}_{\Lambda_\theta}[f], \theta \in \mathbb{R}$ . We compare the Fourier transform with the FrFT in Fig. 1. As shown in Fig. 2(a), the action of the FrFT on the time-frequency co-ordinates  $\mathbf{r} = [t \ \omega]^\top, \mathbf{r} \in \mathbb{R}([0, 1]^2)$  results in rotation of the time-frequency plane [69] due to  $\hat{\mathbf{r}} = \Lambda_\theta \mathbf{r}, \theta \in \mathbb{R}$ —an intrinsic property of the FrFT. This is explained by the co-ordinate transformation matrix—the rotation matrix  $\Lambda_\theta$  in case of the FrFT (cf Table I).

The submatrix  $\Lambda_L$  of  $\Lambda_S$  may be decomposed in several ways. One interesting decomposition relates  $\Lambda_L$  to the Fourier transform such that  $\Lambda_L = \mathbf{M}_1 \Lambda_{\text{FT}} \mathbf{M}_2$  where

$$\mathbf{M}_1 = \begin{bmatrix} b & 0 \\ d & 1/b \end{bmatrix} \quad \text{and} \quad \mathbf{M}_2 = \begin{bmatrix} 1 & 0 \\ a/b & 1 \end{bmatrix}$$

are modulation matrices<sup>1</sup>. This decomposition implies that the SAFT can be implemented as a Fourier

<sup>1</sup>We refer to  $\mathbf{M}_1$  and  $\mathbf{M}_2$  as modulation matrices because whenever  $b = 0$  in (2), the SAFT in (1) amounts to modulation of the function  $f$ .

transform using the following sequence of steps,

$$\begin{aligned} f_1(x) &\stackrel{\text{def}}{=} \mathcal{T}_{\mathbf{M}_2|\mathbf{0}}[f](x) \stackrel{(1)}{=} e^{j\frac{a}{2b}x^2} f(x), \\ \widehat{f}_1(\xi) &= \mathcal{T}_{\Lambda_{\text{Fr}}}[f_1](\xi) = \int f_1(x) e^{-j\xi x} dx, \\ \widehat{f}_1(\omega) &\stackrel{\text{def}}{=} \mathcal{T}_{\mathbf{M}_1|\lambda}[\widehat{f}_1](\omega) \stackrel{(1)}{=} \frac{1}{\sqrt{b}} e^{j\omega q + j\frac{d}{2b}(\omega-p)^2} \widehat{f}_1\left(\frac{\omega-p}{b}\right). \end{aligned}$$

By simplifying  $\widehat{f}_1(\omega)$ , we observe that it is indeed the SAFT of  $f(t)$ . In this way, we generalize the previously known result of Zayed [70] that links the FrFT to the Fourier Transform.

An alternative decomposition relates the SAFT with the FrFT and the Fresnel transform via the elegant Iwasawa Decomposition,

$$\Lambda_{\mathbf{L}} = \Lambda_{\theta} \begin{bmatrix} \Gamma & 0 \\ 0 & \Gamma^{-1} \end{bmatrix} \underbrace{\begin{bmatrix} 1 & u \\ 0 & 1 \end{bmatrix}}_{\text{Fresnel Transform}}, \quad \begin{aligned} \Gamma &= \sqrt{a^2 + c^2} \\ u &= (ab + cd)/\Gamma^2 \end{aligned}.$$

In fact, rotation is a special operation of a class of matrices that belong to the special linear group  $\text{SL}_2(\mathbb{R})$  where,

$$\text{SL}_2(\mathbb{R}) = \left\{ \mathbf{A} = \begin{bmatrix} a_1 & a_2 \\ a_3 & a_4 \end{bmatrix} \left\{ a_k \right\}_{k=1}^4 \in \mathbb{R} \text{ and } |\mathbf{A}| = 1 \right\}.$$

With the exception of the Laplace, Gauss and Bargmann transforms in Table I, all other operations can be explained by  $\Lambda_{\mathbf{L}} \in \text{SL}_2(\mathbb{R})$  which entails that  $ad - bc = 1$ . Since the basis vectors of  $\Lambda_{\mathbf{L}}$  form a parallelogram in  $\mathbb{R}^2$ , its enclosed area must always be unity or the area must be preserved under application of  $\Lambda_{\mathbf{L}}$ . This aspect has important consequences in ray optics where  $\Lambda_{\mathbf{L}}$  models paraxial optics [66], [68]. In Figs. 2(b), 2(c) and 2(d) we describe the deformation on  $\mathbf{r}$  due to  $\Lambda_{\mathbf{S}}$  for the Fresnel transform ( $\Lambda_{\mathbf{S}} = \Lambda_{\text{Fr}}$ ), the LCT ( $\Lambda_{\mathbf{S}} = \Lambda_{\mathbf{L}}$ ) and the SAFT.

Geometrically, the inverse transform relies on specification of  $\Lambda_{\mathbf{S}}^{\text{inv}}$  which undoes the effect of  $\Lambda_{\mathbf{S}}$ . For the FrFT, the Fresnel transform and the LCT, the operation is simply the inverse of the matrix,

that is  $\Lambda_S^{\text{inv}} = \Lambda_S^{-1}$ ,  $\Lambda_S = \{\Lambda_\theta, \Lambda_{\text{Fr}}, \Lambda_L\}$  (cf. Table I). The case of the SAFT is unique because it implements an affine transform as opposed to the usual case of a linear transform (cf. compare Fig. 2(b,c) and Fig. 2(d)). The presence of an offset  $\lambda = [p \ q]^\top$  in (2) warrants an adjustment by  $-\Lambda_L^{-1}\lambda$  (6) for the SAFT.

#### D. Convolution Structures in the SAFT Domain

A useful property of the Fourier transform is that the convolution of two functions is equal to the pointwise multiplication of their spectrums. More precisely,  $\mathcal{T}_{\Lambda_{\text{FT}}}[f * g] = \mathcal{T}_{\Lambda_{\text{FT}}}[f] \mathcal{T}_{\Lambda_{\text{FT}}}[g]$ . However, this property does not extend to the SAFT domain in that  $\mathcal{T}_{\Lambda_S}[f * g] \neq \mathcal{T}_{\Lambda_S}[f] \mathcal{T}_{\Lambda_S}[g]$  (cf. [71]). Since convolutions are pivotal to the topic of sampling theory, we will work with a generalized version of the convolution operator, denoted by  $*_{\Lambda_S}$ , which allows for a representation of the form  $\mathcal{T}_{\Lambda_S}[f *_{\Lambda_S} g] \propto \mathcal{T}_{\Lambda_S}[f] \mathcal{T}_{\Lambda_S}[g]$ .

**Definition 1** (Chirp Modulation). *Let  $\mathbf{A} = [a_{j,k}]$  be a  $2 \times 2$  matrix. We define the chirp modulation function as,*

$$m_{\mathbf{A}}(t) \stackrel{\text{def}}{=} \exp\left(j \frac{a_{11}}{2a_{12}} t^2\right). \quad (9)$$

We also define the  $\mathbf{A}$ -parametrized unitary up and down chirp modulation operation,

$$\vec{f}(t) \stackrel{\text{def}}{=} m_{\mathbf{A}}(t) f(t) \quad \text{and} \quad \overleftarrow{f}(t) \stackrel{\text{def}}{=} m_{\mathbf{A}}^*(t) f(t), \quad (10)$$

respectively. Note that  $\|\vec{f}(t)\|_{L_2}^2 = \|f(t)\|_{L_2}^2$ .

Based on the definition of chirp modulated functions, we now define the SAFT convolution operator.

**Definition 2** (SAFT Convolution). *Let  $*$  denote the usual convolution operator. Given functions  $f$  and  $g$ , the SAFT convolution operator denoted by  $*_{\Lambda_S}$ , is defined as*

$$h(t) = (f *_{\Lambda_S} g)(t) \stackrel{\text{def}}{=} K_b m_{\Lambda_S}^*(t) \left( \vec{f} * \overleftarrow{g} \right)(t), \quad (11)$$

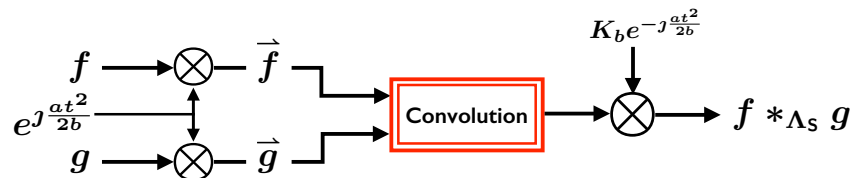


Fig. 3. Block diagram for SAFT convolution. We use the usual definition of the convolution operation in conjunction with chirp modulation defined in (10) to define the SAFT convolution operation.

where  $\vec{f}(t) = m_{\Lambda_S}(t) f(t) \stackrel{(10)}{=} e^{j \frac{at^2}{2b}} f(t)$ ; the same applies to the function  $g$ .

In Fig. 3, we explain the SAFT convolution operation defined in (11). Note that the SAFT convolution operation is based on the usual convolution of pre-modulated functions  $\vec{f}(t)$  and  $\vec{g}(t)$ . This operation, also known as *chirping*, is a standard procedure in optical information processing [72] and analog processing where it is implemented via mixing circuits (cf. Fig. 6(a) in [48]). Similarly, in the field of holography, such operations are used for defining Fresnel transforms (cf. (10) in [50]). Pre- and post-modulations are critical in our context and enforce the convolution-multiplication property. A formal statement of this result is as follows:

**Theorem 1** (Convolution and Product Theorem [63], [65]). *Let  $f$  and  $g$  be two given functions and let  $h(t) = (f *_{\Lambda_S} g)(t)$  be defined in (11). Then,*

$$h(t) \xrightarrow{\text{SAFT}} \widehat{h}_{\Lambda_S}(\omega) = \Phi_{\Lambda_S}(\omega) \widehat{f}_{\Lambda_S}(\omega) \widehat{g}_{\Lambda_S}(\omega),$$

where  $\widehat{f}_{\Lambda_S}(\omega)$ ,  $\widehat{g}_{\Lambda_S}(\omega)$  and  $\widehat{h}_{\Lambda_S}(\omega)$  denote the SAFT of  $f$ ,  $g$  and  $h$ , respectively and  $\Phi_{\Lambda_S}(\omega) = e^{j \frac{\omega}{b}(dp-bq)} e^{-j \frac{d\omega^2}{2b}}$ .

The proof of this theorem is presented in [63]. For further results, we refer the reader to [65]. The duality principle also holds for the SAFT. Namely, multiplication of functions in the time domain results in convolution in the SAFT domains,

$$\Phi_{\Lambda_S^{\text{inv}}}(t) f(t) g(t) \xrightarrow{\text{SAFT}} K_{\Lambda_S^{\text{inv}}} \left( \widehat{f} *_{\Lambda_S^{\text{inv}}} \widehat{g} \right) (\omega)$$

where  $K_{\Lambda_S^{inv}}$  is defined in (7). This result is based on the proof of Theorem 1. For further details, we refer the reader to [65].

### III. SAFT DOMAIN AND BANDLIMITED SUBSPACES

In order to set the ground for sampling of sparse signals, we begin by recalling the sampling theorem for SAFT bandlimited signals [2], [63]. The notion of bandlimitedness has a de facto association with the Fourier domain. Below, we consider a more general definition.

**Definition 3** (Bandlimited Functions). *Let  $f$  be a square-integrable function. We say that  $f$  is  $\Omega_m$ -bandlimited and write,*

$$f \in \mathcal{B}_{\Lambda_S}^{\Omega_m} \Leftrightarrow f(t) = K_{\Lambda_S^{inv}} \int_{-\Omega_m}^{+\Omega_m} \hat{f}_{\Lambda_S}(\omega) \kappa_{\Lambda_S^{inv}}^*(\omega) d\omega.$$

With  $\Lambda_S = \Lambda_{FT}$ , we obtain the standard case when  $f$  is  $\Omega_m$ -bandlimited in the Fourier domain.

Shannon's sampling theorem is restricted to Fourier transforms. In that case,  $\Lambda_S = \Lambda_{FT}$  and any  $f \in \mathcal{B}_{\Lambda_{FT}}^{\Omega_m}$  can be uniquely recovered from samples  $f(k\Delta)$ ,  $k \in \mathbb{Z}$  provided that  $\Delta \leq \pi/\Omega_m$ . For bandlimited signals in the SAFT sense, the statement of Shannon's sampling theorem is follows.

**Theorem 2** (Shannon's Sampling Theorem for the SAFT Domain [63]). *Let  $f$  be an  $\Omega_m$ -bandlimited function in the SAFT domain, that is,  $f \in \mathcal{B}_{\Lambda_S}^{\Omega_m}$ . Then, we have,*

$$f(t) = e^{-J\frac{at^2}{2b}} \sum_{n \in \mathbb{Z}} \vec{f}(n\Delta) e^{-Jp\frac{t-n\Delta}{b}} \text{sinc}_{\Delta}(t-n\Delta).$$

A detailed proof of this theorem that is based on reproducing kernel Hilbert spaces is given in [63]. Here, we will briefly revisit the key steps. The associated computations will be useful in the context of sampling sparse signals.

It is well known that the sampling theorem for the Fourier domain can be interpreted as an orthogonal



projection of  $f$  onto the subspace of bandlimited functions [21],

$$V_{\text{BL}} = \text{span} \left\{ \frac{1}{\sqrt{\Delta}} \text{sinc}_{\Delta}(t - n\Delta) \right\}_{n \in \mathbb{Z}}. \quad (12)$$

Thanks to the projection theorem,

$$\mathcal{P}_{V_{\text{BL}}} f = \arg \min_{g \in V_{\text{BL}}} \|f - g\|_{L_2}^2, \quad f \in \mathcal{B}_{\Lambda_{\text{FT}}}^{\Omega_m} \Leftrightarrow f = \mathcal{P}_{V_{\text{BL}}} f. \quad (13)$$

In the spirit of the Fourier domain result, in [63], we derived the subspace of bandlimited functions linked with the SAFT domain which take the form of,

$$\phi_n(t) = \frac{e^{-j\frac{a}{b}(t-n\Delta)}}{\sqrt{\Delta}} m_{\Lambda_s}^*(t) m_{\Lambda_s}(n\Delta) \text{sinc}_{\Delta}(t - n\Delta). \quad (14)$$

The family  $\{\phi_n(t)\}_{n \in \mathbb{Z}}$  is an orthonormal basis for the subspace of bandlimited functions in the SAFT domain. Indeed,  $\phi_0 \in \mathcal{B}_{\Lambda_s}^{\Omega_m}$  with  $\Omega_m = \pi b/\Delta$  since,

$$\widehat{\phi_0}_{\Lambda_s}(\omega) = \sqrt{\Delta} K_{\Lambda_s} \Phi_{\Lambda_s}^*(\omega) \underbrace{\mathbb{1}_{[-\Omega_m, \Omega_m]}(\omega)}_{\text{Bandlimited}}, \quad \Omega_m = \frac{\pi b}{\Delta}.$$

Thanks to the orthonormality and the bandlimitedness properties, the implication of the projection theorem (cf. (13)) is that  $f \in \mathcal{B}_{\Lambda_s}^{\Omega_m} \Leftrightarrow f = \mathcal{P}_{V_{\text{BL}}} f$  and by developing this further, we obtain,

$$\begin{aligned} \mathcal{P}_{V_{\text{BL}}} f &= \sum_{n \in \mathbb{Z}} \langle f, \phi_n \rangle \phi_n(t) \\ &= e^{-j\frac{at^2}{2b}} \sum_{n \in \mathbb{Z}} \vec{f}(n\Delta) e^{-j\mathcal{P}\frac{t-n\Delta}{b}} \text{sinc}_{\Delta}(t - n\Delta). \end{aligned} \quad (15)$$

As in the classical case, the coefficients  $\{\langle f, \phi_n \rangle\}_n$  are equivalent to low-pass filtering in the SAFT domain followed by uniform sampling. To make this link clear, consider the kernel,

$$\varphi_{\text{BL}}(t) = \frac{1}{\sqrt{\Delta} K_b} m_{\Lambda_s}^*(t) e^{-j\frac{a}{b}t} \text{sinc}_{\Delta}(-t), \quad (16)$$

which is the amplitude scaled version of  $\phi_0$ . Using the convolution-product duality in Theorem 1, it

is easy to verify [63] that  $\forall f \in \mathcal{B}_{\Lambda_s}^{\Omega_m}$ ,

$$\langle f, \phi_n \rangle = \sqrt{\Delta} (f *_{\Lambda_s} \varphi_{\text{BL}})(t)|_{t=n\Delta}, \quad \varphi_{\text{BL}} = K_{\Lambda_s} \phi_0 \quad (17)$$

and the expansion coefficients in (15) are indeed the samples.

#### IV. SPARSE SAMPLING AND SUPER-RESOLUTION

When  $\varphi$  is bandlimited in the Fourier domain, the super-resolution problem boils down to estimating  $\{c_k\}$ 's and  $\{t_k\}$ 's from measurements  $y(n\Delta)$ ,  $\Delta > 0$  of,

$$y(t) = \sum_{k=0}^{K-1} c_k \varphi(t - t_k). \quad (18)$$

This problem can be restated as that of sampling spikes or sparse functions given a bandlimited sampling kernel,  $\varphi$ . This is because of the equivalence,

$$y(n\Delta) = \underbrace{\int s(t) \bar{\varphi}(t - n\Delta) dt}_{\text{Projection}} \equiv \underbrace{(s * \varphi)(t)|_{t=n\Delta}}_{\text{Convolution}}, \quad (19)$$

where  $\bar{\varphi}(t) = \varphi(-t)$ ,  $\Delta > 0$  is the sampling rate and  $s$  is the sparse signal,

$$s(t) = \sum_{k=0}^{K-1} c_k \delta(t - t_k). \quad (20)$$

In the previous section, we discussed sampling theory of bandlimited signals in the SAFT domain. By considering sparse signals instead of bandlimited functions, the measurements in context of the SAFT domain amount to,

$$s \rightarrow \boxed{\varphi} \rightarrow \underbrace{s *_{\Lambda_s} \varphi}_{\text{Pre-Filtering}} = y \rightarrow \underbrace{\otimes_{\delta_{n\Delta}}}_{\text{Sampling}} \rightarrow y(n\Delta), \quad (21)$$

where  $\otimes_{\delta_{n\Delta}}$  denotes the sampling operation or modulation with a  $\Delta$ -periodic impulse train. As shown in (15), whenever  $s \in \mathcal{B}_{\Lambda_s}^{\Omega_m}$ , samples  $y(n\Delta)$  uniquely characterize  $s$  provided that  $\Delta \leq \pi b / \Omega_m$ .

Next, we turn our attention to the problem of recovering a sparse signal from low-pass projections (17). In particular, we will discuss three variations on this theme where low-pass projections are attributed to:

- 1) Arbitrary, bandlimited sampling kernels.
- 2) Smooth, time-limited sampling kernels.
- 3) Gabor functions associated with the SAFT domain.

The first two results rely on the architecture of (21). The last result generalizes the recent work of Aubel *et al.* [73] and can be extended to the case of phase-retrieval [74]–[76] and wavelets.

Since sparse signals are time-limited, their periodic extension allows for a Fourier series representation. That said, the basis functions of the SAFT kernel are aperiodic. As a result, before discussing the recovery of sparse signals, we introduce mathematical tools that allow for Fourier series-like representation of time-limited signals.

#### A. Special Affine Fourier Series (SAFS)

It is well known that the family of functions  $\{e^{jk\omega_0 t}\}_{k \in \mathbb{Z}}$ , with fundamental harmonic  $\omega_0 = 2\pi/T$ , constitutes an orthonormal basis of  $L_2([-\pi/T, \pi/T])$ . These basis functions are used for representing  $T$ -periodic functions. Let  $V_{FS} = \text{span}\{e^{jk\omega_0 t}\}_{k \in \mathbb{Z}}$ . Due to the orthonormality and completeness properties, it follows that, for every  $f(t) = f(t + T)$ ,

$$\mathcal{P}_{V_{FS}} f = \sum_{n \in \mathbb{Z}} c_n e^{jn\omega_0 t}, \quad c_n = \langle f, e^{jn\omega_0 t} \rangle. \quad (22)$$

Inspired by the Fourier series representation, here, we develop a parallel for the SAFT domain which is useful for the task of representing time-limited signals including sparse signals.

In order to determine the basis functions associated with the Special Affine Fourier Series or the SAFS, we first identify the candidate functions and then enforce the orthonormality property. Note

that a spike at frequency  $\omega = n\omega_0$  in the SAFT domain results in the time domain function

$$\left\langle \delta(\omega - n\omega_0), \kappa_{\Lambda_s^{\text{inv}}}(\omega, t) \right\rangle \stackrel{(7)}{=} \kappa_{\Lambda_s^{\text{inv}}}^*(n\omega_0, t). \quad (23)$$

With the above as our prototype basis function, we would like to represent a time-limited signal  $s(t)$ ,  $t \in [0, T)$  as

$$s(t) = \sum_{n \in \mathbb{Z}} \widehat{s}_{\Lambda_s} [n] \kappa_{\Lambda_s^{\text{inv}}}^*(n\omega_0, t), \quad (24)$$

which mimics (22), and where the SAFS coefficients are

$$\widehat{s}_{\Lambda_s} [n] = \langle s, \kappa_{\Lambda_s}(\cdot, n\omega_0) \rangle_{[0, T]}. \quad (25)$$

To enable a representation in the form (25), we enforce orthogonality on the candidate basis functions,

$$\left\langle \kappa_{\Lambda_s}(t, n\omega_0), \kappa_{\Lambda_s^{\text{inv}}}(k\omega_0, t) \right\rangle_{[0, T]} \equiv \underbrace{I_{\omega_0} = w_0 \delta[n - k]}_{\text{Orthogonality}},$$

for an appropriate  $w_0$ . Computing the inner-product explicitly yields,

$$\begin{aligned} I_{\omega_0} &= |K_{\Lambda_s}|^2 \mu \int_0^T e^{j \frac{\omega_0(k-n)}{b} t} dt \\ &= |K_{\Lambda_s}|^2 \begin{cases} T & k = n, \\ -\mu \frac{jb}{(k-n)\omega_0} \left(1 - e^{-j \frac{\omega_0 T}{b} (k-n)}\right) & k \neq n, \end{cases} \end{aligned}$$

where for brevity we denoted,

$$\mu = \left( e^{-j \frac{\omega_0(k-n)}{2b}} (2bq + d\omega_0(k+n) - 2dp) \right).$$

Therefore, the orthogonality property will hold, if,

$$1 - e^{-j \frac{\omega_0 T}{b} (k-n)} = 0 \Leftrightarrow \omega_0 = 2\pi b/T.$$

We consolidate our result in the following definition.

**Definition 4** (Special Affine Fourier Series). *Let  $s$  be a time-limited signal supported on the interval  $[0, T)$ . The Special Affine Fourier Series representation of  $s$  is defined in (24) and (25) where  $\omega_0 = 2\pi b/T$ .*

In case of  $\Lambda_S = \Lambda_{FT}$ , the SAFS reduces to the Fourier series. To see this, let us substitute the parameters of  $\Lambda_{FT}$ , from Table I, in  $\Lambda_S$ . Then, we have,  $\kappa_{\Lambda_S}^*(n\omega_0, t) = e^{jn\omega_0 t}$  which are indeed the basis functions for the Fourier Series (upto a constant,  $K_{\Lambda_S}$ ). Similarly, with  $\Lambda_S = \Lambda_\theta$ , the SAFS reduces to Fractional Fourier series (cf. (10) in [77]).

Based on the definition of the SAFS for time-limited functions, we now develop an alternative representation of sparse signals defined in (20) that are supported on the interval

$$T = \left| \max\{t_k\}_{k=0}^{K-1} - \min\{t_k\}_{k=0}^{K-1} \right|.$$

With  $T$  above and  $\epsilon > 0$ , we compute the SAFS coefficients,

$$\begin{aligned} \widehat{s}_{\Lambda_S}[n] &\stackrel{(25)}{=} \langle s, \kappa_{\Lambda_S}(t, n\omega_0) \rangle \\ &= \int_{\epsilon}^{\epsilon+T} s(t) \kappa_{\Lambda_S}^*(t, n\omega_0) dt \\ &= \sum_{k=0}^{K-1} c_k \kappa_{\Lambda_S}^*(t_k, n\omega_0), \quad \omega_0 = 2\pi b/T. \end{aligned} \tag{26}$$

From (24) we obtain the SAFT series,

$$s(t) \stackrel{(24)}{=} \sum_{n \in \mathbb{Z}} \sum_{k=0}^{K-1} c_k \kappa_{\Lambda_S}^*(t_k, n\omega_0) \kappa_{\Lambda_S}^*(n\omega_0, t). \tag{27}$$

Using (3) we have,

$$\kappa_{\Lambda_S}^*(t_k, n\omega_0) \kappa_{\Lambda_S}^*(n\omega_0, t) \stackrel{(3)}{=} e^{-j(Q(t)-Q(t_k))} e^{j\frac{\omega_0 n}{b}(t-t_k)} \tag{28}$$

where  $Q(t)$  is a quadratic polynomial,

$$Q(t) \stackrel{\text{def}}{=} (at^2 + 2pt) / 2b. \quad (29)$$

Substituting into (27) leads to,

$$\begin{aligned} s(t) &= e^{-jQ(t)} \sum_{n \in \mathbb{Z}} \sum_{k=0}^{K-1} \underbrace{c_k e^{jQ(t_k)}}_{c'_k} \underbrace{e^{-j\frac{\omega_0 n t k}{b}}}_{u_k^n} e^{j\frac{\omega_0 n t}{b}} \\ &= e^{-jQ(t)} \sum_{n \in \mathbb{Z}} \hat{h}[n] e^{j\frac{\omega_0 n t}{b}} \\ &= e^{-jQ(t)} h(t), \end{aligned} \quad (30)$$

where  $\hat{h}[n]$  is a sum of complex exponentials:

$$\hat{h}[n] = \sum_{k=0}^{K-1} c_k e^{jQ(t_k)} e^{-j\frac{\omega_0 n t_k}{b}} = \sum_{k=0}^{K-1} c'_k u_k^n. \quad (31)$$

By arranging (30), we may rewrite,

$$\underbrace{s(t) e^{jQ(t)}}_{h(t)} = \underbrace{\sum_{n \in \mathbb{Z}} \hat{h}[n] e^{j\frac{2\pi}{T} n t}}_{\text{Fourier Series}} \equiv h(t), \quad (32)$$

with  $\hat{h}[n]$  given in (31). We have thus shown that a modulated version of the sparse signal  $s(t)$  is equivalent to another sparse signal,

$$h(t) = \sum_{n \in \mathbb{Z}} \sum_{k=0}^{K-1} c'_k \delta(t - t'_k - nT) \quad (33)$$

where unknowns  $\{c'_k, t'_k\}_{k=0}^{K-1}$  of  $h(t)$  are related to the unknowns of the sparse signal we seek to recover

$$c'_k = c_k e^{jQ(t_k)} \quad \text{and} \quad t'_k = t_k.$$

Due to this link between  $s(t)$  in (20) and  $h(t)$  in (33), their Fourier series coefficients are also related

$$\begin{bmatrix} g_0 \\ \vdots \\ g_{N-1} \end{bmatrix} = \begin{bmatrix} 1 & \cdots & 1 & \cdots & 1 \\ e^{-j\frac{2\pi}{T}f_c} & \ddots & 1 & \ddots & e^{+j\frac{2\pi}{T}f_c} \\ \vdots & \ddots & 1 & \ddots & \vdots \\ e^{-j\frac{2\pi}{T}f_c(N-1)} & \cdots & 1 & \cdots & e^{+j\frac{2\pi}{T}f_c(N-1)} \end{bmatrix} \begin{bmatrix} \hat{h}[-f_c] \\ \vdots \\ \hat{h}[f_c] \end{bmatrix} \equiv \mathbf{g} = \mathbf{V}\hat{\mathbf{h}} \quad (41)$$


---

to one another as in (32). We formally state this result as a theorem.

**Theorem 3** (SAFS of Sparse Signals). *Let  $s(t)$  be the sparse signal defined in (20). Then, the Special Affine Fourier Series representation of  $s(t)$  is given by,*

$$s(t) = e^{-jQ(t)} \sum_{n \in \mathbb{Z}} \hat{h}[n] e^{j\frac{\omega_0 n t}{b}},$$

where  $\hat{h}[n] = \sum_{k=0}^{K-1} c_k e^{jQ(t_k)} e^{-j\frac{\omega_0 n}{b} t_k}$  and  $Q(t)$  is defined in (29).

This re-parameterization of the sparse signal  $s(t)$  in form of the Fourier series coefficients of  $h(t)$  is key to studying sparse sampling theorems in the SAFT domain.

### B. Sparse Signals and Arbitrary Bandlimited Kernels

Consider the setting in which the sampling kernel  $\varphi = \varphi_{\text{BL}}(t)$  (16). In this case, the low-pass filtered measurements are given by  $y(t) = (s *_{\Lambda_s} \varphi_{\text{BL}})(t)$ . The measurements can be expressed in terms of low-pass, orthogonal projections (17) as given in the following proposition.

**Proposition 1** (Bandlimited Case). *Let  $s$  be the sparse signal defined in (20) and the bandlimited sampling kernel  $\varphi_{\text{BL}}(t)$  be defined in (16). Then, the measurements simplify to*

$$y(t) = \sqrt{\Delta} e^{-jQ(t)} \sum_{|m| \leq M} \hat{h}[m] e^{j\frac{\omega_0 m t}{b}}, \quad M = \lfloor \frac{T}{2\Delta} \rfloor, \quad (34)$$

where  $Q$  is defined in (29) and  $\hat{h}[n]$  is defined in (31).

We prove a more general version of this proposition in Section VI-A. Next, we state the main result linked with sampling of sparse signals in the SAFT domain.

**Theorem 4** (Sparse Sampling with Bandlimited Kernel). *Let  $s(t)$  be a continuous-time, sparse signal (20) and let  $\varphi_{\text{LP}}$  be the low-pass filter defined in (16) with  $\Delta = \pi b/\Omega_m$ . Suppose that we observe low-pass filtered samples  $y(n\Delta) = (s *_{\Lambda_S} \varphi_{\text{LP}})(n\Delta)$ ,  $n = 0, \dots, N-1$ . Provided that  $K$  and  $\Lambda_S$  are known and  $N \geq T/\Delta + 1$ , the low-pass filtered samples  $y(n\Delta)$ ,  $n = 0, \dots, N-1$  are a sufficient characterization of the sparse signal  $s(t)$  in (20).*

*Proof.* To show that this statement holds, we start with the observation that modulating the low-pass samples results in the Fourier series of the sparse signal in (33). More precisely,

$$g_n = \frac{y(n\Delta)}{\sqrt{\Delta}} e^{j\mathbf{Q}(n\Delta)} \stackrel{(34)}{=} \sum_{|m| \leq f_c = M} \hat{h}[m] e^{j\frac{\omega_0 m}{b} n\Delta}. \quad (35)$$

Also, from (31), the Fourier coefficients  $\hat{h}[m]$  are a linear combination of complex exponentials. In vector-matrix notation, we have,  $\mathbf{g} = \mathbf{V}\hat{\mathbf{h}}$  (cf. (41)). From (35), we estimate  $\hat{h}[m]$  using the inverse Fourier transform, that is,  $\hat{\mathbf{h}} = \mathbf{V}^+\mathbf{g}$  where  $(\cdot)^+$  denotes the matrix pseudo-inverse. A unique solution to this system of equations exists provided that

$$N \geq 2f_c + 1, \quad f_c = \lfloor T/2\Delta \rfloor. \quad (\text{C1})$$

Having computed  $\hat{\mathbf{h}}$ , we are now left with the task of estimating  $\{c'_k, t'_k\}_{k=0}^{K-1}$  associated with the sparse signal in (33). In spectral estimation theory [78], it is well known that the sum of complex exponentials in (31) admits an autoregressive form which allows us to write,

$$\hat{h}[m] + \sum_{k=1}^K r[k] \hat{h}[m-k] = 0. \quad (36)$$

The  $K$ -tap filter defined by  $\{r[k]\}$  is known as the *annihilating filter* [22], [78] which is used to esti-



mate the non-linear unknowns  $\{t'_k\}_{k=0}^{K-1}$  provided that  $\{t'_k\}_{k=0}^{K-1}$  are distinct and  $\widehat{h}[m]$ ,  $m \in [-K, K]$  is known, thus implying,

$$f_c \geq K. \quad (\text{C2})$$

By combining conditions (C1) and (C2), we finally obtain,

$$N \geq T/\Delta + 1. \quad (37)$$

Whenever (37) holds, a recovery procedure from the FRI literature [22], [23] can be directly applied. To this end, (37) guarantees that we can estimate the filter  $r$  in (36) which is then used for constructing a polynomial of degree  $K$ ,

$$R(z) = \sum_{k=0}^K r[k] z^{-k}.$$

The  $K$ -roots of this polynomial, that is,  $u_k = e^{-j\omega_0 t_k/b}$ , encode the information about  $\{t_k\}_{k=0}^{K-1}$ . Let  $\widetilde{t}_k$  denote the estimate of  $t_k$ . Then, by factorizing  $R(z)$ , we estimate the roots  $\widetilde{u}_k$  which is used to estimate  $\widetilde{t}_k = (b/\omega_0) \angle \widetilde{u}_k$ . To determine  $\{c_k\}_{k=0}^{K-1}$  in (20), we first construct the quadratic polynomial  $Q(\widetilde{t}_k) = (a\widetilde{t}_k^2 + 2p\widetilde{t}_k)/2b$ . There on, we estimate  $\widetilde{c}_k$  by solving the least-squares problem since  $c_k$ 's in (31) linearly depend on known quantities. ■

### C. Generalization to Arbitrary Bandlimited Sampling Kernels

For the same recovery condition (cf. (37)), our result straight-forwardly generalizes to any arbitrary, bandlimited sampling kernel of the form,

$$\psi \in \mathcal{B}_{\Lambda_{\text{FT}}}^{\Omega_m}, \quad \varphi_{\text{BL}}(t) = \frac{1}{\sqrt{\Delta K_b}} m_{\Lambda_s}^*(t) e^{-j\frac{p}{b}t} \psi(\Delta^{-1}t) \quad (38)$$

provided that  $\psi \in \mathcal{B}_{\Lambda_{\text{FT}}}^{\Omega_m}$  and the Fourier transform of  $\psi$  does not vanish in the interval  $[-\Omega_m, \Omega_m]$ . This is a consequence of a generalized version of Proposition 1 (cf. Section VI-A). Arbitrary bandlimited

kernels result in a version of (35),

$$g_n = \sum_{|m| \leq f_c} \hat{h}[m] \hat{\psi} \left( \frac{\omega_0 m \Delta}{b} \right) e^{j \frac{\omega_0 m}{b} n \Delta} \Leftrightarrow \mathbf{g} = \mathbf{V} \mathbf{D} \hat{\mathbf{h}},$$

where  $\mathbf{D}$  is a diagonal matrix composed of Fourier series coefficients of  $\psi$ , that is,  $\{\hat{\psi}(\Delta \omega_0 m/b)\}_{|m| \leq f_c}$ . Given  $\psi$ ,  $\hat{\mathbf{h}}$  can be “deconvolved” using  $\hat{\mathbf{h}} = \mathbf{D}^{-1} \mathbf{V}^+ \mathbf{g}$  (cf. Section I).

#### *D. Special cases of the SAFT domain result*

By appropriately selecting the parameter matrix  $\Lambda_S$ , we can directly derive results for any of the operations described in Table I. Next, we revisit some examples in the literature which are special cases of the SAFT domain.

#### **Sparse or FRI Sampling in Fourier Domain**

The FRI sampling result which was derived in context of Fourier domain [22] is a special case of Theorem 4. By setting,

$$\Lambda_S = \left[ \begin{array}{cc|c} 0 & 1 & 0 \\ -1 & 0 & 0 \end{array} \right] \equiv \Lambda_{FT},$$

we note that  $Q(t) = 0$  and  $s(t) = h(t)$  in (32). In this case the sampling rate is  $\Delta = \pi/\Omega_m$  and provided that  $N \geq T/\Delta + 1$ , the sparse signal can be recovered from low-pass projections in the Fourier domain.

#### **Sparse Sampling in Fractional Fourier Domain**

Sparse sampling in context of the fractional Fourier domain was discussed in [64]. As above, this is a special case of Theorem 4. By setting,

$$\Lambda_S = \left[ \begin{array}{cc|c} \cos \theta & \sin \theta & 0 \\ -\sin \theta & \cos \theta & 0 \end{array} \right] \equiv \Lambda_{\theta},$$

we note that  $Q(t) = \frac{t^2}{2} \cot \theta$  and as shown in [64],  $s(t)$  is given by,

$$s(t) \stackrel{(32)}{=} e^{-j\frac{t^2}{2} \cot \theta} \sum_{n \in \mathbb{Z}} \sum_{k=0}^{K-1} c'_k u_k^n e^{j\frac{2\pi}{T} nt},$$

where  $c'_k = c_k e^{j\frac{t_k^2}{2} \cot \theta}$ . In this case the sampling rate is  $\Delta = \pi \sin \theta / \Omega_m$  and provided that  $N \geq T/\Delta + 1$ , the sparse signal can be recovered from low-pass projections in the Fractional Fourier domain.

### Link with Super-resolution via Convex Programming

Our work is directly related to recent results on super-resolution based on convex-programming [5].

Let,

$$\|s\|_{\text{TV}} = \sum_{k=0}^{K-1} |c_k|$$

denote the TV-norm of the sparse signal  $s$  (20). Also note that,  $\|s\|_{\text{TV}} = \|h\|_{\text{TV}}$ . Given sampled measurements  $\{y(n\Delta)\}_{n=0}^{N-1}$  (34) we first obtain  $\{g_n\}_{n=0}^{N-1}$  from (35). We then estimate  $\hat{\mathbf{h}} = \mathbf{V}^+ \mathbf{g}$ . As a result, we may recast our sparse recovery problem as a minimization problem of the form,

$$\min_h \|h\|_{\text{TV}} \text{ with } \left\{ \hat{h}[m] = \int_0^T h(t) e^{j\omega_0 mt} dt \right\}_{|m| \leq f_c}. \quad (39)$$

Theorem 4 assumes knowledge of  $K$ —a proxy for *sparsity* or the *rate of innovation*. Accordingly, the sampling criterion (37) is based on a counting principle: the kernel bandwidth should be at least equal to the number of unknowns (cf. (C2)). With  $K$  known, in the absence of perturbations, the unknowns  $\{t_k\}_{k=0}^{K-1}$  can be arbitrarily close. In contrast, (39) avoids any assumptions on  $K$  but relies on a minimum separation principle [5].

Let  $\mathbb{T}_K = \{t_k\}_{k=0}^{K-1}$  denote the support of  $s$  and let us define the minimum separation between any two entries of  $\mathbb{T}_K$  by,

$$\delta_{\min}(\mathbb{T}_K) \stackrel{\text{def}}{=} \inf_{\mathbb{T}_K: t_k \neq t_\ell} |t_k - t_\ell|.$$

We can now repurpose our generalized result in the context of super-resolution [5]. The formal result

is as follows.

**Theorem 5** (Exact Recovery based on Minimum Separation Principle). *Let  $\mathbb{T}_K = \{t_k\}_{k=0}^{K-1}$  be the support set of the sparse signal  $s$  and  $f_c = \lfloor T/2\Delta \rfloor$  be the cut-off frequency of the sampling kernel defined in (16). If  $\delta_{\min}(\mathbb{T}_K) f_c \geq 2$  then  $h$  (and hence  $s$ ) is a unique solution to (39).*

The proof of this theorem follows from [5]. Even though our discussion is quite general (due to Table I), extension to [5] comes at no extra cost—the computational complexity and the exact recovery principle remain the same. A similar parallel can be drawn with the work on atomic norms [79].

### E. Sparse Signals and Smooth Time-limited Kernels

In the previous section, we focused on sampling kernels which were bandlimited (38). However, in applications, the sampling kernels may be pulses or echoes that are time-limited [12]–[14], [18], [25], [80]. In this case, we can model such a sampling kernel as a SAFS (24),

$$\begin{aligned} \psi(t) &\stackrel{(24)}{=} \sum_{n \in \mathbb{Z}} \hat{\psi}_{\Lambda_s}[n] \kappa_{\Lambda_s^*}^*(n\omega_0, t), \quad \psi(t) = 0, t \notin [0, T] \\ &= \sum_{n \in \mathbb{Z}} \hat{\psi}_{\Lambda_s}[n] e^{-jQ(t)} \Phi_{\Lambda_s}(n\omega_0) e^{j\frac{n\omega_0 t}{b}}, \end{aligned} \quad (40)$$

where  $\Phi_{\Lambda_s}(\omega) = e^{j\frac{\omega}{b}(dp-bq)} e^{-j\frac{d\omega^2}{2b}}$  and  $Q(t)$  is defined in (29). As usual, the filtered spikes are given by  $y(t) = (s *_{\Lambda_s} \psi)(t)$ . A further simplification of the measurements is due to the following proposition which deals with time-limited kernels.

**Proposition 2** (Time-limited Case). *Let  $s$  be the sparse signal defined in (20) and the time-limited sampling kernel  $\psi(t)$  be defined in (40). Then, the filtered spikes simplify to*

$$y(t) = e^{-jQ(t)} \sum_{m \in \mathbb{Z}} \hat{h}[m] \hat{\psi}_{\Lambda_s}[m] \Phi_{\Lambda_s}(m\omega_0) e^{j\frac{\omega_0 m}{b} t}, \quad (41)$$

where  $Q$  is defined in (29) and  $\hat{h}$  is defined in (31).

This result is proved in Section VI-B. In defining  $\psi$  in (40), time-limitedness was the only assumed property for developing the SAFS representation. In practice one would expect  $\psi$  to be a bounded, smooth function. From Fourier regularity conditions, we know that a function is bounded and  $N$  times continuously differentiable provided that [21],

$$\int |\widehat{\psi}_{\Lambda_{\text{FT}}}(\omega)| (1 + |\omega|^N) d\omega < \infty.$$

In many cases,  $\psi$  is a smooth and compactly supported pulse/function [12], [14], [25]. The next proposition states a sufficient condition for smoothness (or differentiability) of a function  $\psi$  in the SAFT domain.

**Proposition 3.** (*Smoothness and Decay*) *A function  $f$  is bounded and  $N$  times continuously differentiable with bounded derivatives provided that (ignoring constant  $K_{\Lambda_s}$ )*

$$\int \left| [\mathbb{L}(\omega) + a\mathcal{D}]^N \widehat{f}_{\Lambda_s}(\omega) \right| d\omega < \infty,$$

where  $\mathcal{D}$  is the usual derivative operator and  $\mathbb{L}$  is some linear polynomial. The action of  $[\mathbb{L}(\omega) + a\mathcal{D}]^N$  on  $\widehat{f}_{\Lambda_s}$  should be understood in the operator sense.

The proof of this proposition is based on recurrence relations and is presented in Section VI-C. As an example, consider  $N = 1$ . In this case (by using (53) and (56)),  $\mathcal{T}_{\text{SAFT}} : f^{(1)}(t) \rightarrow \mathbb{L}(\omega) \widehat{f}_{\Lambda_s}(\omega) + a\mathcal{D}\widehat{f}_{\Lambda_s}(\omega)$ . In view of this result,

$$\begin{aligned} |\mathcal{D}f(t)| &\leq \int \left| \mathbb{L}(\omega) \widehat{f}_{\Lambda_s}(\omega) + a\mathcal{D}\widehat{f}_{\Lambda_s}(\omega) \right| d\omega \\ &\leq \|\mathbb{L}\widehat{f}_{\Lambda_s}\|_{L_1} + |a| \|\mathcal{D}\widehat{f}_{\Lambda_s}\|_{L_1} < \infty, \end{aligned}$$

where the last result is due to Minkowski's inequality. Note that for  $N = 1$ , both  $\widehat{f}_{\Lambda_s}$  and  $\mathcal{D}\widehat{f}_{\Lambda_s}$  should be in  $L_1$ . For the case of the Fourier transform, we have  $a = 0$  (cf. Table I) and the result collapses to  $|\omega|^N |\widehat{f}_{\Lambda_{\text{FT}}}(\omega)|$ .

The smoothness properties of kernels are of significant interest in the context of sampling and approximation theory [81]. While a detailed discussion is beyond the scope of this work, for sparse sampling, Proposition 3 is enough to establish that  $\widehat{\psi}_{\Lambda_S}$  decays to zero whenever  $\psi$  is a smooth kernel. Consequently, for some  $f_c = M > 0$ , we have  $\widehat{\psi}_{\Lambda_S}[m] = 0, |m| > M$  and therefore,  $M$  dictates the recovery bound for perfect reconstruction of  $s$ . Without loss of generality, by setting  $\Delta = 1$  and,

$$\widehat{\psi}'_{\Lambda_S}[m] \stackrel{\text{def}}{=} \widehat{\psi}_{\Lambda_S}[m] \Phi_{\Lambda_S}(m\omega_0),$$

the samples take the form of

$$g_n \stackrel{(41)}{=} \sum_{|m| \leq M} \widehat{h}[m] \widehat{\psi}'_{\Lambda_S}[m] e^{j\frac{\omega_0 m}{b} n}, n = 0, \dots, N - 1.$$

This problem is similar to the one in Section IV-C and in view of Theorem 4, perfect recovery is guaranteed provided that  $N \geq 2M + 1$  with  $M \geq K$ .

#### F. Sparse Signals and the Gabor Transform Kernel

Several recent works consider recovery of sparse signals from Gabor transform measurements. Aubel *et al.* [73] study this problem in the context of super-resolution. Similarly, Matusiak *et al.* [82] studied the problem of sparse sampling using Gabor frames. Recently, Eldar *et al.* [74] developed algorithms for recovery of sparse signals in the context of the phase retrieval. Uniqueness guarantees with respect to phase retrieval problem for the Gabor transform were reported by Jaganathan *et al.* in [83]. In all of these cases, the results were developed for the Fourier domain ( $\Lambda_S = \Lambda_{FT}$ ). Here, we generalize the sparse recovery problem to the SAFT domain. For this purpose, we introduce the Gabor transform associated with the SAFT domain together with some basic mathematical properties.

**Definition 5** (Gabor Transform for the SAFT Domain). *Let  $f$  be a function with well defined SAFT and  $\psi \in L_2$  be some window. We define the SAFT Gabor transform (SAFT-GT) by,*

$$\widehat{S}_{\Lambda_S}^{f,\psi}(\tau, \omega) = \int f(t) \psi(t - \tau) \kappa_{\Lambda_S}^*(t, \omega) dt. \quad (42)$$

Next, we derive the inversion formula linked with the SAFT domain. Without loss of generality, we assume that  $K_{\Lambda_s} = 1$ .

**Proposition 4** (Inversion Formula for the SAFT-GT). *Let  $f$  be some function with a well defined SAFT and  $\psi_1, \psi_2 \in L_2$  be window functions. Furthermore, let  $\widehat{S}_{\Lambda_s}^{f, \psi_1}(\tau, \omega)$  denote the SAFT-GT of  $f$  defined in (42). Provided that  $b \langle \psi_1, \psi_2 \rangle = 1$ , the inverse SAFT-GT is defined by,*

$$f(t) = \iint_{\tau, \omega} \widehat{S}_{\Lambda_s}^{f, \psi_1}(\tau, \omega) \psi_2(t - \tau) \kappa_{\Lambda_s}^* \text{inv}(\omega, t) d\omega d\tau. \quad (43)$$

A proof of this proposition is presented in Section VI-D.

In the context of the SAFT-GT, the sparse signal (20), or alternatively (30), can be represented as,

$$y(\tau, \omega) \stackrel{(42)}{=} \underbrace{\Phi_{\Lambda_s}^*(\omega) \sum_{k=0}^{K-1} c'_k \psi(t_k - \tau) e^{-j \frac{\omega}{b} t_k}}_{\widehat{S}_{\Lambda_s}^{s, \psi}(\tau, \omega)}. \quad (44)$$

Let  $y'(t, \omega) = y(t, \omega) \Phi(\omega)$  where  $\Phi_{\Lambda_s}$  is a modulation operation with  $\Phi_{\Lambda_s} \Phi_{\Lambda_s}^* = 1$ .

$$y'(t, \omega) \stackrel{\text{def}}{=} \sum_{k=0}^{K-1} c'_k \psi(t_k - t) e^{-j \frac{\omega}{b} t_k}. \quad (45)$$

Since  $\psi$  is a known, smooth window, a finite Fourier series approximation—time scaled by  $b$ —suffices to approximate  $\psi$ ,

$$\widetilde{\psi}_M(t) \approx \sum_{|m| \leq M} \widehat{\psi}_{\Lambda_{\text{FT}}}[m] \kappa_{\Lambda_{\text{FT}}}^*(t, \omega_0 m/b), \quad \omega_0 = 2\pi b/T.$$

Let  $M = f_c$  and assume sampled measurements of the form,

$$y(\tau, \omega) \Big|_{\tau=n\Delta}^{\omega=\ell\omega_0}, \quad (\tau, \omega) \in [0, N-1] \times [-f_c, f_c].$$

Next, we study the recovery of  $s$  in two separate cases:

■ **Case 1: Recovery with a fixed  $\omega$ .**

By fixing  $\omega = \omega_0$  and  $\psi \rightarrow \psi_M$ ,

$$y(n\Delta, \omega_0) = \underbrace{\Phi_{\Lambda_S}^*(\omega_0)}_{\text{Constant}} \sum_{k=0}^{K-1} \underbrace{c'_k e^{-j\frac{\omega_0}{b}t_k}}_{\check{c}_k} \psi_M(t_k - n\Delta)$$

where the weights reflect the effect of the SAFT,  $\check{c}_k \stackrel{\text{def}}{=} c'_k e^{-j\frac{\omega_0}{b}t_k} = c_k e^{jQ(t_k)} e^{-j\frac{\omega_0}{b}t_k}$ . Finally, note that this is the classical sparse sampling problem (cf. compare (18)),

$$y'(n\Delta, \omega_0) = \sum_{k=0}^{K-1} \check{c}_k \bar{\psi}_M(n\Delta - t_k)$$

where  $\bar{\psi}_M = \psi_M(-\cdot)$  and the result of Section IV-C can be directly extended to the case at hand. Provided that  $f_c = M \geq K$  and  $N \geq 2M + 1$ , perfect recovery is guaranteed.

■ Case 2: Recovery using both  $(\tau, \omega)$ .

From (45) and  $\psi_M \approx \psi$ , we have,

$$\begin{aligned} y'(n\Delta, \ell\omega_0) &= \sum_{k=0}^{K-1} c_k \sum_{|m| \leq M} \hat{\psi}_{\Lambda_{\text{FT}}}[m] e^{j\frac{t_k}{b}(m\omega_0 - \ell\omega_0)} e^{-j\frac{m\omega_0}{b}n\Delta} \\ &= \sum_{|m| \leq M} \check{y}_{m,\ell} e^{-j\frac{m\omega_0}{b}n\Delta} \end{aligned} \quad (46)$$

where,  $\check{y}_{m,\ell} \stackrel{\text{def}}{=} \sum_{k=0}^{K-1} \hat{\psi}_{\Lambda_{\text{FT}}}[m] c_k e^{j\frac{t_k}{b}(m\omega_0 - \ell\omega_0)}$ . This development is the standard form (with regards to the Fourier domain) and the results in [73] can be extended to solve for (46). For a Gaussian window function, the exact recovery principle based on minimum separation condition is discussed in [73] (cf. Theorem 11) and applies to (46).

## V. CONCLUSION

In this work, we considered the recovery of sparse signals from their low-pass/bandlimited projections in the SAFT domain. Since the SAFT parametrically generalizes a number of interesting transformations listed in Table I, our work presents a unifying approach to the problem of sampling



and recovery of sparse signals. Starting with a review of Shannon's sampling theorem for signals that are bandlimited in the SAFT domain, we developed conditions for exact recovery of sparse signals when, (1) sampling with arbitrary, bandlimited kernels, (2) sampling with smooth, time-limited kernels and, (3) recovery from Gabor transform measurements linked with the SAFT domain. By setting  $\Lambda_S = \Lambda_{FT}$  and  $\Lambda_\theta$ , our results coincide with previously discussed results linked with the Fourier and Fractional Fourier domain, respectively.

## VI. APPENDIX: AUXILIARY PROOFS AND COMPUTATIONS

### A. Proof of Proposition 1

Here, we will prove a more general result. Let  $\psi$  be an arbitrary function with a well defined Fourier transform and let  $\varphi(t) = (\Delta K_b^2)^{-1/2} m_{\Lambda_S}^*(t) e^{-j\frac{p}{b}t} \psi(t)$ . By using the definition of the SAFT-convolution (11), we have

$$\begin{aligned}
 y(t) &= K_{\Lambda_S} m_{\Lambda_S}^*(t) \left( \vec{s} * \vec{\varphi} \right) (t) \\
 &\stackrel{(a)}{=} \Delta_c m_{\Lambda_S}^*(t) \left( e^{j\frac{p}{b}t} h(t) * e^{j\frac{p}{b}t} \psi(t) \right) \\
 &\stackrel{(b)}{=} \Delta_c m_{\Lambda_S}^*(t) e^{j\frac{p}{b}t} (h(t) * \psi(t)) \\
 &\stackrel{(c)}{=} \Delta_c e^{-jQ(t)} \sum_{m \in \mathbb{Z}} \hat{h}[m] \hat{\psi} \left( \frac{\omega_0 m}{b} \right) e^{j\frac{\omega_0 m}{b} t}, \tag{47}
 \end{aligned}$$

where  $\Delta_c = 1/\sqrt{\Delta}$ , (a) is due to (11), (b) is due to invariance of complex exponentials under convolution operation (eigen-function property) and (c) is because  $h$  is a  $T$ -periodic function (33). Here,  $y(t)$  is completely characterized by the Fourier series coefficients of  $h$  and  $\psi$ . With  $\psi(t) = \text{sinc}_\Delta(t)$ , we have,  $\hat{\psi}(\omega) = \Delta \mathbb{1}_{[-\frac{\pi}{\Delta}, \frac{\pi}{\Delta}]}(\omega)$  where  $\omega = \omega_0 m/b$  and since  $\hat{\psi}(m\omega_0\Delta/b) = 0, m > T/2\Delta$ , (34) holds.

*B. Proof of Proposition 2*

We will start by developing  $\vec{s} * \vec{\psi}$  which appears in the definition of the convolution operator (11).

Note that,

$$\begin{aligned}\vec{s}(t) &= e^{-J_b^p t} h(t), \quad \text{and} \\ \vec{\psi}(t) &= e^{-J_b^p t} \sum_{n \in \mathbb{Z}} \hat{\psi}_{\Lambda_s}[n] \Phi_{\Lambda_s}(n\omega_0) e^{J_b^{\omega_0} t}.\end{aligned}$$

By letting  $\hat{z}[n] \stackrel{\text{def}}{=} \hat{\psi}_{\Lambda_s}[n] \Phi(n\omega_0)$ , we may re-write  $\vec{\psi}(t)$  in terms of Fourier series of  $z(t)$ ,

$$\vec{\psi}(t) = e^{-J_b^p t} \sum_{n \in \mathbb{Z}} \hat{z}[n] e^{J_b^{\omega_0} t} \equiv e^{-J_b^p t} z(t).$$

Based, on this, we now develop,

$$\begin{aligned}(\vec{s} * \vec{\psi})(t) &= e^{-J_b^p t} h(t) * e^{-J_b^p t} z(t) \\ &\stackrel{\text{(a)}}{=} e^{-J_b^p t} (h * z)(t) \\ &\stackrel{\text{(b)}}{=} e^{-J_b^p t} T \sum_{m \in \mathbb{Z}} \hat{h}[m] \hat{z}[m] e^{J_b^{\omega_0} t},\end{aligned}$$

where (a) is due to invariance of complex exponentials under convolution operation (eigen-function property) and (b) is due to convolution-product theorem for the Fourier series. For simplicity, let us assume that  $TK_{\Lambda_s} = 1$ . Then, we have,

$$\begin{aligned}y(t) &= K_{\Lambda_s} m_{\Lambda_s}^*(t) e^{-J_b^p t} T \sum_{m \in \mathbb{Z}} \hat{h}[m] \hat{z}[m] e^{J_b^{\omega_0} t}, \\ &= e^{-J_b^p t} \sum_{m \in \mathbb{Z}} \hat{h}[m] \hat{\psi}_{\Lambda_s}[m] \Phi(m\omega_0) e^{J_b^{\omega_0} t},\end{aligned} \tag{48}$$

which completes our proof.

*C. Proof of Proposition 3*

In order to prove this result, we begin with the observation,

$$\left| f^{(k)}(t) \right| = \left| \int F_k(\omega) \kappa_{\Lambda_S^*}^*(\omega, t) d\omega \right| \leq \int |F_k(\omega)| d\omega < \infty, \quad (49)$$

where  $F_k(\omega)$ , expressed as a function of  $\widehat{f}_{\Lambda_S}(\omega)$ , is the SAFT of  $f^{(k)}(t)$  which is yet to be determined. In analogy to the Fourier transform,  $F_k(\omega) \propto (j\omega)^k \widehat{f}_{\Lambda_{FT}}(\omega)$ . To set up this proof, we will start with defining smooth functions. Let  $f$  be some function with norm defined as  $\forall m, n \in \mathbb{Z}_+ \cup \{0\}, \|f\|_{m,n} = \sup_{t \in \mathbb{R}} |t^m f^{(n)}(t)|$ . Then, we say  $f$  is smooth or  $f \in \mathcal{S}$  provided that  $\|f\|_{m,n} < \infty$ . For functions  $u$  and  $v$  bounded in this norm, integration by parts results in,

$$\int u^{(1)}(t) v(t) dt = - \int u(t) v^{(1)}(t) dt. \quad (50)$$

Let  $u(t) \stackrel{\text{def}}{=} f^{(k)}(t)$  and  $v(\mathbf{r}) \stackrel{\text{def}}{=} \kappa_{\Lambda_S^*}(\mathbf{r})$  where  $\mathbf{r} = [t \ \omega]^\top$ . Also note two useful relations that will be used shortly,

$$\partial_t v(\mathbf{r}) = \beta(p - \omega + at) v(\mathbf{r}) \quad (51)$$

$$\partial_\omega v(\mathbf{r}) = \beta((d\omega - \mu) - t) v(\mathbf{r}), \quad \mu \stackrel{\text{def}}{=} dp - bq, \quad (52)$$

where  $\beta = j/b$ . Next, with  $Z_0(\omega) \stackrel{\text{def}}{=} \widehat{f}_{\Lambda_S}(\omega)$ , let us define a sequence of functions  $\{Z_k\}, k \in \mathbb{Z}_+ \cup \{0\}$ ,

$$Z_k(\omega) \stackrel{\text{def}}{=} \int f^{(k)}(t) v(t, \omega) dt \equiv \int f^{(k)}(t) \kappa_{\Lambda_S^*}(t, \omega) dt. \quad (53)$$

Similarly, we also define  $\{X_k\}, k \in \mathbb{Z}_+ \cup \{0\}$ ,

$$X_k(\omega) \stackrel{\text{def}}{=} \int t f^{(k)}(t) v(t, \omega) dt.$$

Thanks to the sequences  $\{Z_k, X_k\}$ , (50) can be reduced to the following recursive form,

$$Z_{k+1}(\omega) \stackrel{(50)}{=} \beta(\omega - p) Z_k(\omega) - a\beta X_k(\omega). \quad (54)$$

Our result relies on  $Z_k$  and hence, we must eliminate  $X_k$ . We do so by observing that,

$$\begin{aligned}
 Z_k^{(1)}(\omega) &= \int f^{(k)}(t) \underbrace{\partial_\omega v(t, \omega)}_{\text{Replace by (52)}} dt \\
 &= \int f^{(k)}(t) \beta((d\omega - \mu) - t) v(t, \omega) dt \\
 &= \beta(d\omega - \mu) Z_k(\omega) - \beta X_k(\omega).
 \end{aligned} \tag{55}$$

We now solve for  $Z_k$  from the system of equations (54), (55),

$$\begin{bmatrix} Z_{k+1}(\omega) \\ Z_k(\omega) \end{bmatrix} = \beta \begin{bmatrix} \omega - p & -a \\ d\omega - \mu & 1 \end{bmatrix} \begin{bmatrix} Z_k(\omega) \\ X_k(\omega) \end{bmatrix}$$

which leads to a simple recursive equation,

$$\begin{aligned}
 Z_{k+1}(\omega) &= L(\omega) Z_k(\omega) + a Z_k^{(1)}(\omega), \\
 &= [L(\omega) + a\mathcal{D}] Z_k(\omega)
 \end{aligned}$$

where  $L(\omega)$  is linear polynomial  $L(\omega) = \beta(\omega bc + a\mu - p)$  with  $\mu = dp - bq$  and is completely characterized by  $\Lambda_S$ . Now since  $Z_0(\omega) = \widehat{f}_{\Lambda_S}(\omega)$ , we observe that,

$$Z_k(\omega) = [L(\omega) + a\mathcal{D}]^k \widehat{f}_{\Lambda_S}(\omega), \quad Z_0(\omega) = \widehat{f}_{\Lambda_S}(\omega) \tag{56}$$

and by definition (53),  $F_k = Z_k$ . Back substituting  $Z_k$  in (49) leads to the result of Proposition 3.

#### D. Proof of Proposition 4

Let us assume (43) is true. Furthermore, we have,

$$\left\langle \kappa_{\Lambda_S}^*(x, \omega), \kappa_{\Lambda_S}^{\text{inv}}(\omega, t) \right\rangle = e^{J(Q(x) - Q(t))} \underbrace{\int e^{-J\frac{\omega}{b}(x-t)} d\omega}_{b\delta(x-t)}. \tag{57}$$

Next, we substitute  $\widehat{S}_{\Lambda_S}^{f,\psi}(\tau, \omega)$  in (43) to obtain,

$$\iint_{\tau, x} f(x) \psi_1(x - \tau) \psi_2(x - \tau) \left\langle \kappa_{\Lambda_S}^*(x, \omega), \kappa_{\Lambda_S}^{\text{inv}}(\omega, t) \right\rangle dx d\tau.$$

Thanks to (57), by marginalizing  $\omega$  and then  $x$ , the last equation yields  $bf(t) \langle \psi_1, \psi_2 \rangle = I_f$ . Setting  $I_f = f$  verifies the result.

## REFERENCES

- [1] A. Bhandari, Y. C. Eldar, and R. Raskar, "Super-resolution in phase space," in *IEEE Intl. Conf. on Acoustics, Speech and Signal Processing (ICASSP)*, Apr. 2015, pp. 4155–4159.
- [2] A. Bhandari and Y. C. Eldar, "A swiss army knife for finite rate of innovation sampling theory," in *IEEE Intl. Conf. on Acoustics, Speech and Signal Processing (ICASSP)*, Mar. 2016, pp. 3999 – 4003.
- [3] D. L. Donoho, "Superresolution via sparsity constraints," *SIAM Journal on Mathematical Analysis*, vol. 23, no. 5, pp. 1309–1331, Sep. 1992.
- [4] T. Manabe and H. Takai, "Superresolution of multipath delay profiles measured by PN correlation method," *IEEE Trans. Antennas Propag.*, vol. 40, no. 5, pp. 500–509, May 1992.
- [5] E. J. Candès and C. Fernandez-Granda, "Towards a mathematical theory of super-resolution," *Communications on Pure and Applied Mathematics*, vol. 67, no. 6, pp. 906–956, Apr. 2013.
- [6] J. J. Fuchs and H. Chuberre, "A deconvolution approach to source localization," *IEEE Trans. Sig. Proc.*, vol. 42, no. 6, pp. 1462–1470, Jun. 1994.
- [7] H. Zi-qiang and W. Zhen-dong, "A new method for high resolution estimation of time delay," in *IEEE Intl. Conf. on Acoustics, Speech and Signal Processing (ICASSP)*, vol. 7, May 1982, pp. 420–423.
- [8] M. A. Pallas and G. Jourdain, "Active high resolution time delay estimation for large BT signals," *IEEE Trans. Sig. Proc.*, vol. 39, no. 4, pp. 781–788, Apr. 1991.
- [9] J. Li and R. Wu, "An efficient algorithm for time delay estimation," *IEEE Trans. Sig. Proc.*, vol. 46, no. 8, pp. 2231–2235, Aug. 1998.
- [10] K. Gedalyahu and Y. C. Eldar, "Time-delay estimation from low-rate samples: A union of subspaces approach," *IEEE Trans. Sig. Proc.*, vol. 58, no. 6, pp. 3017–3031, Jun. 2010.
- [11] L. Li and T. P. Speed, "Parametric deconvolution of positive spike trains," *Annals of Statistics*, pp. 1279–1301, 2000.
- [12] S. Hernandez-Marin, A. Wallace, and G. Gibson, "Bayesian analysis of lidar signals with multiple returns," *IEEE Trans. Pattern Anal. Mach. Intell.*, vol. 29, no. 12, pp. 2170–2180, Dec. 2007.

- [13] A. Bhandari, A. Kadambi, and R. Raskar, “Sparse linear operator identification without sparse regularization? Applications to mixed pixel problem in time-of-flight/range imaging,” in *IEEE Intl. Conf. on Acoustics, Speech and Signal Processing (ICASSP)*, May 2014, pp. 365–369.
- [14] A. Bhandari and R. Raskar, “Signal processing for time-of-flight imaging sensors,” *IEEE Signal Process. Mag.*, vol. 33, no. 4, pp. 2–16, Sep. 2016.
- [15] O. Bar-Ilan and Y. C. Eldar, “Sub-nyquist radar via doppler focusing,” *IEEE Trans. Sig. Proc.*, vol. 62, no. 7, pp. 1796–1811, Apr. 2014.
- [16] S. Rudresh and C. S. Seelamantula, “Finite-rate-of-innovation-sampling-based super-resolution radar imaging,” *IEEE Trans. Sig. Proc.*, vol. 65, no. 19, pp. 5021–5033, Oct. 2017.
- [17] A. Bhandari and T. Blu, “FRI sampling and time-varying pulses: Some theory and four short stories,” in *IEEE Intl. Conf. on Acoustics, Speech and Signal Processing (ICASSP)*, Mar. 2017.
- [18] R. Tur, Y. C. Eldar, and Z. Friedman, “Innovation rate sampling of pulse streams with application to ultrasound imaging,” *IEEE Trans. Sig. Proc.*, vol. 59, no. 4, pp. 1827–1842, Apr. 2011.
- [19] A. Burshtein, M. Birk, T. Chernyakova, A. Eilam, A. Kempinski, and Y. C. Eldar, “Sub-nyquist sampling and Fourier domain beamforming in volumetric ultrasound imaging,” *IEEE Trans. Ultrason., Ferroelectr., Freq. Control*, vol. 63, no. 5, pp. 703–716, May 2016.
- [20] M. Unser, “Sampling—50 years after Shannon,” *Proc. IEEE*, vol. 88, no. 4, pp. 569–587, 2000.
- [21] Y. C. Eldar, *Sampling Theory: Beyond Bandlimited Systems*. Cambridge University Press, 2015.
- [22] M. Vetterli, P. Marziliano, and T. Blu, “Sampling signals with finite rate of innovation,” *IEEE Trans. Sig. Proc.*, vol. 50, no. 6, pp. 1417–1428, 2002.
- [23] T. Blu, P. L. Dragotti, M. Vetterli, P. Marziliano, and L. Coulot, “Sparse sampling of signal innovations,” *IEEE Signal Process. Mag.*, vol. 25, no. 2, pp. 31–40, 2008.
- [24] Y. Barbotin, A. Hormati, S. Rangan, and M. Vetterli, “Estimation of sparse MIMO channels with common support,” *IEEE Trans. Commun.*, vol. 60, no. 12, pp. 3705–3716, Dec. 2012.
- [25] A. Bhandari, A. M. Wallace, and R. Raskar, “Super-resolved time-of-flight sensing via FRI sampling theory,” in *IEEE Intl. Conf. on Acoustics, Speech and Signal Processing (ICASSP)*, Mar. 2016.
- [26] S. Deslauriers-Gauthier and P. Marziliano, “Sampling signals with a finite rate of innovation on the sphere,” *IEEE Trans. Sig. Proc.*, vol. 61, no. 18, pp. 4552–4561, 2013.
- [27] C. Chen, P. Marziliano, and A. C. Kot, “2D finite rate of innovation reconstruction method for step edge and polygon signals in the presence of noise,” *IEEE Trans. Sig. Proc.*, vol. 60, no. 6, pp. 2851–2859, Jun. 2012.
- [28] H. Pan, T. Blu, and P. L. Dragotti, “Sampling curves with finite rate of innovation,” *IEEE Trans. Sig. Proc.*, vol. 62, no. 2, pp. 458–471, Jan. 2014.

- [29] S. Mulleti and C. S. Seelamantula, "Ellipse fitting using the finite rate of innovation sampling principle," *IEEE Trans. Image Proc.*, vol. 25, no. 3, pp. 1451–1464, Mar. 2016.
- [30] J. Oñativia, S. R. Schultz, and P. L. Dragotti, "A finite rate of innovation algorithm for fast and accurate spike detection from two-photon calcium imaging," *J. Neural Eng.*, vol. 10, no. 4, p. 046017, Jul. 2013.
- [31] Z. Dogan, T. Blu, and D. V. D. Ville, "Detecting spontaneous brain activity in functional magnetic resonance imaging using finite rate of innovation," in *IEEE Intl. Symp. on Biomed. Imaging*. IEEE, Apr. 2014.
- [32] C. S. Seelamantula and S. Mulleti, "Super-resolution reconstruction in frequency-domain optical-coherence tomography using the finite-rate-of-innovation principle," *IEEE Trans. Sig. Proc.*, vol. 62, no. 19, pp. 5020–5029, Oct. 2014.
- [33] H. Pan, T. Blu, and M. Vetterli, "Towards generalized FRI sampling with an application to source resolution in radioastronomy," *IEEE Trans. Sig. Proc.*, vol. 65, no. 4, pp. 821–835, Feb. 2017.
- [34] S. Mulleti, A. Singh, V. P. Brahmkhatri, K. Chandra, T. Raza, S. P. Mukherjee, C. S. Seelamantula, and H. S. Atreya, "Super-resolved nuclear magnetic resonance spectroscopy," *Scientific Reports*, vol. 7, no. 1, Aug. 2017.
- [35] A. Bhandari, F. Kraemer, and Ramesh, "On unlimited sampling," in *Intl. Conf. on Sampling Theory and Applications (SampTA)*, Jul. 2017.
- [36] A. Bhandari, F. Kraemer, and R. Raskar, "Unlimited sampling of sparse signals," in *IEEE Intl. Conf. on Acoustics, Speech and Signal Processing (ICASSP)*, Apr. 2018.
- [37] J. Murray-Bruce and P. L. Dragotti, "A sampling framework for solving physics-driven inverse source problems," *IEEE Trans. Sig. Proc.*, vol. 65, no. 24, pp. 6365–6380, Dec. 2017.
- [38] H. Pan, R. Scheibler, E. F. Bezzam, I. Dokmanic, and M. Vetterli, "FRIDA: Fri-based doa estimation for arbitrary array layouts," in *IEEE Intl. Conf. on Acoustics, Speech and Signal Processing (ICASSP)*, 2017.
- [39] S. Peleg and B. Porat, "Estimation and classification of polynomial-phase signals," *IEEE Trans. Inf. Theory*, vol. 37, no. 2, pp. 422–430, Mar. 1991.
- [40] X. Yuan, "Estimating the DOA and the polarization of a polynomial-phase signal using a single polarized vector-sensor," *IEEE Trans. Sig. Proc.*, vol. 60, no. 3, pp. 1270–1282, Mar. 2012.
- [41] A. Amar, "Efficient estimation of a narrow-band polynomial phase signal impinging on a sensor array," *IEEE Trans. Sig. Proc.*, vol. 58, no. 2, pp. 923–927, Feb. 2010.
- [42] S. Mann and S. Haykin, "The chirplet transform: physical considerations," *IEEE Trans. Sig. Proc.*, vol. 43, no. 11, pp. 2745–2761, 1995.
- [43] R. Baraniuk and D. Jones, "Shear madness: new orthonormal bases and frames using chirp functions," *IEEE Trans. Sig. Proc.*, vol. 41, no. 12, pp. 3543–3549, 1993.
- [44] R. Gribonval, "Fast matching pursuit with a multiscale dictionary of Gaussian chirps," *IEEE Trans. Sig. Proc.*, vol. 49, no. 5, pp. 994–1001, 2001.

- [45] G. Engen and Y. Larsen, "Efficient full aperture processing of TOPS mode data using the moving band chirp  $z$ -transform," *IEEE Trans. Geosci. Remote Sensing*, vol. 49, no. 10, pp. 3688–3693, Oct. 2011.
- [46] S. Schock, "A method for estimating the physical and acoustic properties of the sea bed using chirp sonar data," *IEEE Journal of Oceanic Engineering*, vol. 29, no. 4, pp. 1200–1217, Oct. 2004.
- [47] M. Martone, "A multicarrier system based on the fractional Fourier transform for time-frequency-selective channels," *IEEE Trans. Commun.*, vol. 49, no. 6, pp. 1011–1020, Jun. 2001.
- [48] A. Harms, W. U. Bajwa, and R. Calderbank, "Identification of linear time-varying systems through waveform diversity," *IEEE Trans. Sig. Proc.*, vol. 63, no. 8, pp. 2070–2084, Apr. 2015.
- [49] F. Gori, "Fresnel transform and sampling theorem," *Optics Communications*, vol. 39, no. 5, pp. 293–297, Nov. 1981.
- [50] N. Chacko, M. Liebling, and T. Blu, "Discretization of continuous convolution operators for accurate modeling of wave propagation in digital holography," *Journal of the Optical Society of America A*, vol. 30, no. 10, p. 2012, Sep. 2013.
- [51] S.-C. Pei and J.-J. Ding, "Relations between Gabor transforms and fractional Fourier transforms and their applications for signal processing," *IEEE Trans. Sig. Proc.*, vol. 55, no. 10, pp. 4839–4850, Oct. 2007.
- [52] I. Yetik and A. Nehorai, "Beamforming using the fractional Fourier transform," *IEEE Trans. Sig. Proc.*, vol. 51, no. 6, pp. 1663–1668, Jun. 2003.
- [53] T. Setälä, T. Shirai, and A. T. Friberg, "Fractional Fourier transform in temporal ghost imaging with classical light," *Physical Review A*, vol. 82, no. 4, Oct. 2010.
- [54] G. Unnikrishnan, J. Joseph, and K. Singh, "Optical encryption by double-random phase encoding in the fractional Fourier domain," *Optics Letters*, vol. 25, no. 12, p. 887, Jun. 2000.
- [55] Y. Huang, "Entropic uncertainty relations in multidimensional position and momentum spaces," *Physical Review A*, vol. 83, no. 5, May 2011.
- [56] E. U. Condon, "Immersion of the Fourier transform in a continuous group of functional transformations," *Proceedings of the National Academy of Sciences*, vol. 23, no. 3, pp. 158–164, Mar. 1937.
- [57] M. Moshinsky and C. Quesne, "Linear canonical transformations and their unitary representations," *Journal of Mathematical Physics*, vol. 12, no. 8, pp. 1772–1780, 1971.
- [58] J. J. Healy, M. A. Kutay, H. M. Ozaktas, and J. T. Sheridan, Eds., *Linear Canonical Transforms: Theory and Applications*, ser. Springer Series in Optical Sciences. Springer New York, 2016, vol. 198.
- [59] L. B. Almeida, "The fractional Fourier transform and time-frequency representations," *IEEE Trans. Sig. Proc.*, vol. 42, no. 11, pp. 3084–3091, 1994.
- [60] R. Tao, B. Deng, W.-Q. Zhang, and Y. Wang, "Sampling and sampling rate conversion of band limited signals in the fractional Fourier transform domain," *IEEE Trans. Sig. Proc.*, vol. 56, no. 1, pp. 158–171, Jan. 2008.



- [61] A. Bhandari and A. I. Zayed, "Shift-invariant and sampling spaces associated with the fractional Fourier transform domain," *IEEE Trans. Sig. Proc.*, vol. 60, no. 4, pp. 1627–1637, 2012.
- [62] J. Shi, X. Liu, X. Sha, and N. Zhang, "Sampling and reconstruction of signals in function spaces associated with the linear canonical transform," *IEEE Trans. Sig. Proc.*, vol. 60, no. 11, pp. 6041–6047, Nov. 2012.
- [63] A. Bhandari and A. I. Zayed, "Shift-invariant and sampling spaces associated with the special affine Fourier transform," *Applied and Computational Harmonic Analysis*, Jul. 2017.
- [64] A. Bhandari and P. Marziliano, "Sampling and reconstruction of sparse signals in fractional Fourier domain," *IEEE Signal Process. Lett.*, vol. 17, no. 3, pp. 221–224, 2010.
- [65] A. Bhandari and A. I. Zayed, *Frontiers In Orthogonal Polynomials And Q-series*. World Scientific, 2018, ch. Convolution and Product Theorem for the Special Affine Fourier Transform, pp. 119–137.
- [66] S. Abe and J. T. Sheridan, "Generalization of the fractional Fourier transformation to an arbitrary linear lossless transformation an operator approach," *J. of Physics A: Math. and General*, vol. 27, no. 12, p. 4179, 1994.
- [67] S. C. Pei and J. J. Ding, "Eigenfunctions of Fourier and fractional Fourier transforms with complex offsets and parameters," *IEEE Trans. Circuits Syst. I*, vol. 54, no. 7, pp. 1599–1611, Jul. 2007.
- [68] A. Gerrard and J. Burch, *Introduction to Matrix Methods in Optics*, ser. Dover Books on Physics. Dover, 1975.
- [69] M. J. Bastiaans and A. J. Van Leest, "From the rectangular to the quincunx Gabor lattice via fractional Fourier transformation," *IEEE Signal Process. Lett.*, vol. 5, no. 8, pp. 203–205, Aug. 1998.
- [70] A. I. Zayed, "On the relationship between the Fourier and fractional Fourier transforms," *IEEE Signal Process. Lett.*, vol. 3, no. 12, pp. 310–311, Dec. 1996.
- [71] Q. Xiang and K. Qin, "Convolution, correlation, and sampling theorems for the offset linear canonical transform," *Signal, Image and Video Processing*, pp. 1–10, 2012.
- [72] H. M. Ozaktas, D. Mendlovic, L. Onural, and B. Barshan, "Convolution, filtering, and multiplexing in fractional Fourier domains and their relation to chirp and wavelet transforms," *Journal of the Optical Society of America A*, vol. 11, no. 2, p. 547, Feb. 1994.
- [73] C. Aubel, D. Stotz, and H. Bölcskei, "A theory of super-resolution from short-time Fourier transform measurements," *Journal of Fourier Analysis and Applications*, 2017.
- [74] Y. C. Eldar, P. Sidorenko, D. G. Mixon, S. Barel, and O. Cohen, "Sparse phase retrieval from short-time Fourier measurements," *IEEE Signal Process. Lett.*, vol. 22, no. 5, pp. 638–642, May 2015.
- [75] Z. Zalevsky, R. G. Dorsch, and D. Mendlovic, "Gerchberg-Saxton algorithm applied in the fractional Fourier or the Fresnel domain," *Optics Letters*, vol. 21, no. 12, p. 842, Jun. 1996.
- [76] B.-Z. Dong, Y. Zhang, B.-Y. Gu, and G.-Z. Yang, "Numerical investigation of phase retrieval in a fractional Fourier transform," *Journal of the Optical Society of America A*, vol. 14, no. 10, p. 2709, Oct. 1997.

- [77] S.-C. Pei, M.-H. Yeh, and T.-L. Luo, “Fractional Fourier series expansion for finite signals and dual extension to discrete-time fractional Fourier transform,” *IEEE Trans. Sig. Proc.*, vol. 47, no. 10, pp. 2883–2888, 1999.
- [78] R. L. Stoica, P. and Moses, *Introduction to spectral analysis*. Prentice hall Upper Saddle River, 1997, vol. 1.
- [79] B. N. Bhaskar, G. Tang, and B. Recht, “Atomic norm denoising with applications to line spectral estimation,” *IEEE Trans. Sig. Proc.*, vol. 61, no. 23, pp. 5987–5999, Dec. 2013.
- [80] A. Bhandari, C. Barsi, and R. Raskar, “Blind and reference-free fluorescence lifetime estimation via consumer time-of-flight sensors,” *Optica*, vol. 2, no. 11, p. 965, Nov. 2015.
- [81] T. Blu and M. Unser, “Quantitative Fourier analysis of approximation techniques: Part I—Interpolators and projectors,” *IEEE Trans. Sig. Proc.*, vol. 47, no. 10, pp. 2783–2795, Oct. 1999.
- [82] E. Matusiak and Y. C. Eldar, “Sub-Nyquist sampling of short pulses,” *IEEE Trans. Sig. Proc.*, vol. 60, no. 3, pp. 1134–1148, Mar. 2012.
- [83] K. Jaganathan, Y. C. Eldar, and B. Hassibi, “STFT phase retrieval: Uniqueness guarantees and recovery algorithms,” *IEEE J. Sel. Topics Signal Process.*, vol. 10, no. 4, pp. 770–781, Jun. 2016.